Journal of Mathematical Biology (2021) 82:59
https://doi.org/10.1007/s00285-021-01612-3

Mathematical Biology

A delay model for persistent viral infections in replicating cells

Hayriye Gulbudak[1] · Paul L. Salceanu[1] · Gail S. K. Wolkowicz[2]

Received: 16 March 2020 / Revised: 13 April 2021 / Accepted: 21 April 2021 / Published online: 15 May 2021

Abstract

Persistently infecting viruses remain within infected cells for a prolonged period of time without killing the cells and can reproduce via budding virus particles or passing on to daughter cells after division. The ability for populations of infected cells to be long-lived and replicate viral progeny through cell division may be critical for virus survival in examples such as HIV latent reservoirs, tumor oncolytic virotherapy, and non-virulent phages in microbial hosts. We consider a model for persistent viral infection within a replicating cell population with time delay in the eclipse stage prior to infected cell replicative form. We obtain reproduction numbers that provide criteria for the existence and stability of the equilibria of the system and provide bifurcation diagrams illustrating *transcritical (backward and forward), saddle-node, and Hopf* bifurcations, and provide evidence of *homoclinic bifurcations* and a *Bogdanov–Takens bifurcation*. We investigate the possibility of long term survival of the infection (represented by chronically infected cells and free virus) in the cell population by using the mathematical concept of *robust uniform persistence*. Using numerical continuation software with parameter values estimated from phage-microbe systems, we obtain two parameter bifurcation diagrams that divide parameter space into regions with different dynamical outcomes. We thus investigate how varying different parameters, including how the time spent in the eclipse phase, can influence whether or not the virus survives.

Keywords Persistent viral infection · Chronically infecting phage · Stability analysis · Bistable dynamics · Backward bifurcation · Robust uniform persistence · Bogdanov–Takens bifurcation

Mathematics Subject Classification 92C50 Medical applications (general) · 92D25 Populations dynamics · 37G35 Dynamical aspects of attractors and their bifurcations · 37N25 dynamical systems in biology

✉ Hayriye Gulbudak
hayriye.gulbudak@louisiana.edu

[1] Mathematics Department, University of Louisiana at Lafayette, Lafayette, LA, USA

[2] Department of Mathematics and Statistics, McMaster University, Hamilton, ON, Canada

1 Introduction

Persistent viral infection mode is observed across distinct cell and virus populations. It is mainly characterized by prolonged viral infection without the virus rapidly killing or causing excessive damage to the host cells. The ability for populations of infected cells to be long-lived and replicate viral progeny through cell division may be critical for virus survival in examples such as HIV latent reservoir (Chomont et al. 2009; Rong and Perelson 2009), tumor oncolytic virotherapy (Wodarz 2001), and temperate phages in microbial hosts (Gulbudak and Weitz 2019; Stewart and Levin 1984; Weitz et al. 2019). Yet, despite their importance, persistent viral infections are less studied; in particular for phage-microbe systems. In this paper, we explore how distinct physiological processes, such as the eclipse stage, interact with dual modes of virus reproduction (infected cell division and viral budding), and affects the virus - host cell population dynamics.

The eclipse stage is critical for phage reproductive and microbial cell life history. During this stage microbes can evolve resistance to infection and also acquire immunity to infection (via intracellular defense mechanisms including resistance-modification, CRISPR-Cas, BREX and other systems (Goldfarb et al. 2015; Labrie et al. 2010)) or upon viral entry, a sequential process takes place (such as the translation, transcription, export, etc.), leading to successful infection. Eclipse stage is usually defined for lytic viruses as the span during a phage infection starting with phage adsorption and ending with the maturation of the first phage particle. In order to generalize for temperate (e.g. chronic, lysogenic, latent, carrier) infections, we define the end of the eclipse stage to coincide with initiation of Replicative Form (RF) (Loh et al. 2019), whereby virus reproduction can then occur through passing on to daughter cells or by budding off virions. Different than virulent (lytic) viruses, temperate viruses form a persistent infection where progeny may bud from the cell as the viral genome is passed to daughter cells asymmetrically after division (Díaz-Muñoz and Koskella 2014) prior to inducing lysis or with no lysis. In all settings, the eclipse stage can be relevant in duration and its impact on infection dynamics. For the chronically infecting bacteriophage $M13$, which is known for infecting Escherichia Coli cells, the eclipse stage usually takes 12 minutes after phage induction at $t = 0$, Ploss and Kuhn (2010), relatively significant on the time-scale of the infected cell doubling time. Studies of lytic viral infection have found greater burst sizes are associated with larger latent periods, shorter generation times with shorter latent periods, resulting in evolution of length of eclipse stage, according to host density, and analogous features of the temperate eclipse stage may be important (Abedon et al. 2001).

Mathematical models can provide crucial insights into how distinct mechanisms might affect the dynamics of interacting viral and cell populations. The bulk of population dynamic models of virus-microbe systems focus on the lytic mode (Beretta and Kuang 1998; Childs et al. 2012; Jover et al. 2013; Levin et al. 1977; Smith and De Leenheer 2003; Weitz 2016). Some of these previous studies have extended the standard model to include the time lag between microbial host infection and viral production, but do not consider persistently infected cells (Beretta et al. 2002; Han and Smith 2012; Smith 2011; Smith and Thieme 2012). Gulbudak and Weitz (2019) show that extending to chronic infection mode in the standard model (without delay or

eclipse stage) can lead to more complex bifurcation dynamics, and furthermore induce coexistence with a lytic virus exploiting the same microbial hosts. Here, we consider a delay differential equation system for persistently infecting viruses to investigate how the combined influence of two-fold virus reproduction, cellular competition and eclipse stage can influence the outcomes of the population dynamics.

The model introduced here can be also a groundwork for within-host persistent infections. For example, the variables introduced here for susceptible (S) and infected cells (C) can represent the density of in-host uninfected and infected T-cells and HIV virus, respectively in the context of HIV. In Chomont et al. (2009), experiments show that homeostatic proliferation of latently infected cells contributes to HIV persistence. In Rong and Perelson (2009), Rong and Perelson introduce a model, where uninfected and latently infected cells can replicate, and the later ones pass the infection on to daughter cells after division. In addition, similar models (with no eclipse stage time delay) for persistent infections are also introduced for Hepatitis B (Ciupe and Heffernan 2017; Dahari et al. 2009; Goyal et al. 2017) and tumor oncolytic virotherapy (Wodarz 2001). In experimental studies of these virus infections, the importance of eclipse stage is emphasized (Bai et al. 2019; Ishida et al. 2018; Kakizoe et al. 2015). However rigorous bifurcation analysis of a virus model with replicating infected cells, eclipse stage and time delay has not been conducted. Therefore in this study, we interpret the analytical and numerical results not only in the context of viral infection modes in phage-microbe systems, but also in within-host persistent viral infections such as HIV (Rong and Perelson 2009) and tumor oncolytic virotherapy (Wodarz 2001).

The paper is organized as follows: In Sect. 2, we formulate a time delay model of persistent viruses and their host cells with eclipse stage and time lag in virus production. We establish wellposedness of the system and show that the system is dissipative. In Sect. 3, we find the equilibria and analyze their existence and stability for biologically interpretable threshold conditions. We provide criteria for transcritical bifurcations (both *forward* and *backward*) and demonstate that the model can display bi-stability. We also investigate the possibility of long term survival of the infection by using the mathematical concept of *robust uniform persistence*. In Sect. 4, we provide bifurcation diagrams illustrating the wide range of possible dynamics. In Sect. 5, we discuss the biological implications of our analysis. Finally, in Sect. 6, we summarize our results. In addition, we provide all of the proofs in the Appendix.

2 A time-delay model of persistent viruses

We propose a nonlinear model describing the interactions between chronic viruses, $V(t)$, and their host cells, divided into three subclasses: susceptible host cells $S(t)$; host cells in the eclipse stage upon viral infection, $E(t)$; and the latently (chronically) infected host cells $C(t)$. Time-delay, τ, introduced to model is the length of the time spent in the eclipse phase, the period in which the virus has infected the cell, but has not yet begun to replicate within the cell. In particular, the end of the eclipse stage coincides with initiation of Replicative Form (RF) (Loh et al. 2019), whereby virus reproduction can then occur through passing on to daughter cells or by budding off virions.

In the absence of cell infection, the (susceptible) host cell density grows with logistic growth rate:

$$\frac{dS}{dt} = rS\left(1 - \frac{N}{K}\right) - dS$$

where K represents the carrying capacity for the total cell density, $N = S + E + C$, and r denotes "the net cell growth rate constant," induced by cellular division. The parameter d represents the per capita natural cellular host mortality (in the absence of viral infection). In the presence of viruses, we assume that susceptible cells (S) absorb free viruses (V) at a rate $\phi S(t)V(t)$, and immediately enter the eclipse stage (E). The eclipse phase begins with inoculation when the virions attach to host cells and is assumed to have a fixed duration of τ hours post infection. During this eclipse stage, a sequential process takes place before initiation of Replicative Form (RF), including the translation, transcription, export, etc.. Cells are subject to the natural death rate $\hat{d}$. The cells infected at time $t - \tau$ that survive the eclipse stage, given by $\phi e^{-\hat{d}\tau} S(t-\tau)V(t-\tau)$, transition to the chronic stage (C) after the delay of τ units of time, and then virus reproduction can occur through passing on the virus to daughter cells or by budding off virions, with a rate α, until death. We assume that chronically infecting virus pass down to daughter cells and the infected cells then grow with rate $r_0(1 - \frac{N}{K})$, without lysis at any time.

We obtain the following coupled nonlinear delay differential equation system:

$$\begin{aligned}
\frac{\mathrm{d}S}{\mathrm{d}t} &= rS\left(1 - \frac{N}{K}\right) - \phi SV - dS \\
\frac{\mathrm{d}E}{\mathrm{d}t} &= \phi SV - \hat{d}E - \phi e^{-\hat{d}\tau} S(t-\tau)V(t-\tau) \\
\frac{\mathrm{d}C}{\mathrm{d}t} &= r_0 C\left(1 - \frac{N}{K}\right) - \tilde{d}C + \phi e^{-\hat{d}\tau} S(t-\tau)V(t-\tau) \\
\frac{\mathrm{d}V}{\mathrm{d}t} &= \alpha C - \phi SV - \mu V,
\end{aligned} \tag{1}$$

where μ and $\tilde{d}$ denote the decay/ death rate for viruses and chronically infected cells, respectively. Note that if one assumes that the life cycle of the virus does not involve an eclipse stage, as in model (III) in Gulbudak and Weitz (2019), then $\tau = 0$ in model (1), and the equation for $E(t)$ decouples. If $E(0) > 0$, then $E(t) \to 0$ as $t \to \infty$. However, in that case, it would be more likely that $E(t) = 0$, $t \geq 0$. Introducing the eclipse stage and hence assuming $\tau > 0$ makes the analysis more challenging, since the eclipse stage is not decoupled as opposed to prior delay models because we have $N = S + E + C$ in the logistic terms. The logistic growth terms in the model in the equation of the susceptible and the chronic cell populations include the effect of competition between cells in the susceptible, eclipse, and infected states for limited resources. Due to costly biological processes during the eclipse phase, we also assume that the cells in the eclipse phase cannot replicate.

The *state space* for (1) is the set of functions $\mathcal{D} = \{\Phi = (\Phi_1, \Phi_2, \Phi_3, \Phi_4) \in C_+ \mid \Phi_2(0) = 0 \Rightarrow \Phi_1(0)\Phi_4(0) - \phi e^{-\hat{d}\tau}\Phi_1(-\tau)\Phi_4(-\tau) \geq 0\}$, where $C_+ = \{F : [-\tau, 0] \to \mathbb{R}^4_+ \mid F \text{ is continuous}\}$. This state space is biologically reasonable and with this choice of state space, all solutions with nonnegative initial data remain nonnegative for all subsequent times (see the Appendix A.7 for more details).

Notice that model (1) can be used for other temperate viruses, including lysogenic, carrier, and latently infecting viruses, where both horizontal and vertical transmission (with or without viral budding/lysis) take place (Weitz et al. 2019). Furthermore, the results here also can be applied to lytic virus-host systems, by letting chronically infected cell growth rate r_0 become zero, scaling viral production rate $\alpha = N\tilde{d}$ with burst size N, and either letting $\tilde{d} \to \infty$ for viral bursting or keeping $\tilde{d}$ constant for budding (Smith 2011). Beretta and Kuang (2001) introduced a similar model for lytic viruses. However there are differences between our model and the one in Beretta and Kuang (2001). Our system has both a chronic infected class and an eclipse stage and the dynamics of the infected cells in the eclipse stage is coupled with the rest of our system, in contrast to previous delay models. Finally, the time delay τ, represents the time spent in the eclipse stage prior to transitioning to the chronically infected stage when cell division and viral budding occurs. While these assumptions make the model biologically more reasonable for viruses that result in persistent infections, it also presents mathematical challenges.

3 Thresholds dynamics, bifurcation & persistence analysis

System (1) has multiple *boundary* equilibria: the trivial (community collapse) equilibrium, $\mathcal{E}_0^0 = (0, 0, 0, 0)$; an infection-free equilibrium, $\mathcal{E}_0 = (S_0, 0, 0, 0)$, where $S_0 = K\left(1 - \frac{d}{r}\right)$; and a chronic-only equilibrium, $\mathcal{E}_c$, given by

$$\mathcal{E}_c = (0, 0, C_0, V_c), \quad \text{with} \quad C_0 = K\left(1 - \frac{\tilde{d}}{r_0}\right) \text{ and } V_c = \frac{\alpha}{\mu}C_0. \tag{2}$$

$\mathcal{E}_c$ exists (i.e., is biologically relevant) if and only if $\tilde{d} < r_0$.

System (1) can also have up to two biologically feasible interior equilibria that we will denote by

$$\mathcal{E}_i^\dagger = (S_i^\dagger, E_i^\dagger, C_i^\dagger, V_i^\dagger) \; i = 1, 2$$

when they exist (see Proposition 1).

Now define the *basic reproduction number,* $\mathcal{R}_0$, as follows:

$$\mathcal{R}_0 = \frac{r_0}{\tilde{d}}\left(1 - \frac{S_0}{K}\right) + \frac{\phi S_0}{\phi S_0 + \mu}\frac{\alpha e^{-\hat{d}\tau}}{\tilde{d}}. \tag{3}$$

The threshold quantity $\mathcal{R}_0$ gives the average number of secondary chronically infected cells produced by one chronically infected cell during its life span in a wholly susceptible cell population. The first term, $\frac{r_0}{\tilde{d}}\left(1-\frac{S_0}{K}\right)$, is *the average number of offspring* produced by one chronically infected cell through vertical transmission (chronically infecting viruses passed down to daughter cells) and the second term, $\frac{\phi S_0}{\phi S_0+\mu}\frac{\alpha e^{-\hat{d}\tau}}{\tilde{d}}$, describes the average number of secondary chronically infected cases are produced by one chronically infected cell via horizontal transmission (Gulbudak and Weitz 2019; Weitz et al. 2019).

The trivial community collapse equilibrium, $\mathcal{E}_0^0$, always exists, but is unstable whenever $\mathcal{R}_0^0 > 1$, where $\mathcal{R}_0^0 = \frac{r}{\hat{d}}$. For the rest of the paper, we assume that $\mathcal{R}_0^0 > 1$, unless otherwise stated. This is a necessary and sufficient condition for the existence of the infection-free equilibrium $\mathcal{E}_0 = (S_0, 0, 0, 0)$. Let us define $\mathcal{R}_0^{C_0} = \frac{r_0}{\tilde{d}}$. Note that the chronic-only equilibrium, $\mathcal{E}_c$ exists if and only if $\mathcal{R}_0^{C_0} > 1$.

Next, we state the following local stability results for $\mathcal{E}_0$ and $\mathcal{E}_c$.

Theorem 1 *If $\mathcal{R}_0 < 1$, then $\mathcal{E}_0$ is locally asymptotically stable and if $\mathcal{R}_0 > 1$, then it is unstable.*

The proof is in Appendix A.1

We also define the *susceptible invasion reproduction number* (calculated at the chronic only equilibrium, $\mathcal{E}_c$) as:

$$\mathcal{R}_S^{C_0} = \frac{S_0}{C_0} - \frac{K\phi\alpha}{r\mu}. \tag{4}$$

The following local stability result predicts that if $\mathcal{R}_S^{C_0} < 1$, then when the initial condition sufficiently close to $\mathcal{E}_c$, a subpopulation of chronically infected viruses can outcompete the susceptible resident population; i.e it substitutes the susceptible cell population. However if the inequality is reversed, all cell populations can coexist (See Fig. 1b)).

Theorem 2 *Assume $\mathcal{R}_0^{C_0} > 1$. Then $\mathcal{E}_c$ is locally asymptotically stable if $\mathcal{R}_S^{C_0} < 1$ and it is unstable if $\mathcal{R}_S^{C_0} > 1$.*

The proof is in Appendix A.2.

Next, we consider the interior equilibria, and establish the following result (the proof is given in Appendix A.3):

Proposition 1 *System (1) can have at most two interior equilibria, where each S component of an interior equilibria $\mathcal{E}_i^\dagger = (S_i^\dagger, E_i^\dagger, C_i^\dagger, V_i^\dagger)$, $i = 1, 2$, must satisfy the quadratic equation:*

$$\hat{P}(S) = A_0S^2 + A_1S + A_2 = 0, \tag{5}$$

with

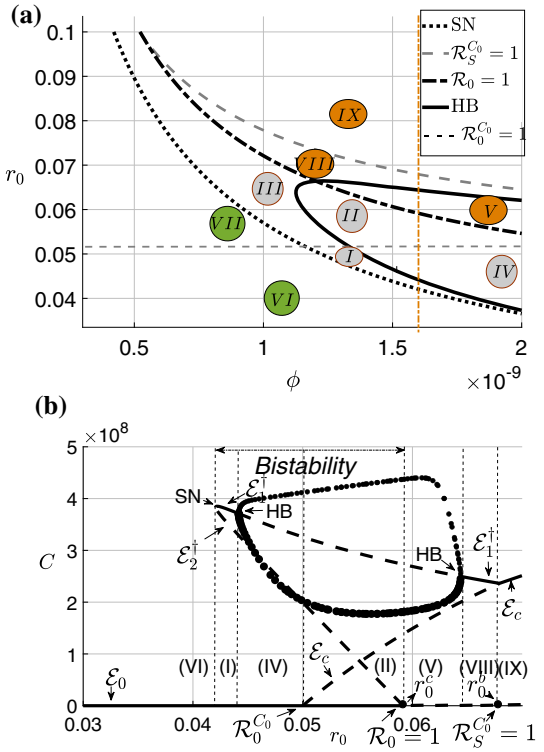

Fig. 1 Bifurcation diagrams for system (1). All parameter values used, apart from the bifurcation parameters, r_0 and ϕ, are given in Table 3, except we set $\tau = 1$ and $\alpha = 1/21$. **a** Two-parameter bifurcation diagram with bifurcation parameters: infection rate, ϕ, and chronic cell net growth rate, r_0. A description of the dynamics in each region, i.e., the invariant sets and their stability, is provided in Table 4. In the regions indicated by green ovals (Regions VI-VII) below the saddle-node bifurcation, the viral infection dies out. In the regions indicated by grey ovals (Regions I-IV) (lying between the curves of the saddle-node bifurcation and the curve where $\mathcal{R}_0 = 1$), the system has two attractors, and display bistable dynamics. Finally the regions indicated by orange ovals (Regions V & VIII-IX) (lying above the curve where $\mathcal{R}_0 = 1$), the system has single attractor and infection persists. **b** The corresponding one-parameter bifurcation diagram along the vertical dash-dotted red line indicated on **a** showing the bifurcation sequence obtained when only r_0 varies and $\phi = 1.6 \times 10^{-9}$. On the one-parameter bifurcation diagram, the solid curves indicate the C component of stable equilibria, dashed curves the C component of unstable equilibria, and filled circles the largest and smallest values of the C component on an orbitally asymptotically stable periodic solution. There is a backward bifurcation at r_0^c involving $\mathcal{E}_0$ and $\mathcal{E}_2^\dagger$ and a forward bifurcation at r_0^h involving $\mathcal{E}_c$ and $\mathcal{E}_1^\dagger$

$$
\begin{aligned}
A_0 &= \frac{\phi}{\alpha r_0}\left[r(\tilde{d}-\alpha e^{-\hat{d}\tau})\left(1-\frac{\alpha(e^{-\hat{d}\tau}-1)}{\hat{d}}\right)+r_0\left(\alpha-d(1-\frac{\alpha(e^{-\hat{d}\tau}-1)}{\hat{d}})\right)\right].\\
A_1 &= \left(\mu\left[B-\frac{re^{-\hat{d}\tau}}{r_0}+1\right]+\mu B\left[1+\frac{\alpha}{\hat{d}}[1-e^{-\hat{d}\tau}]\right]-\frac{\alpha\phi e^{-\hat{d}\tau}K}{r_0}-\phi C_0\right),\\
A_2 &= \frac{\mu^2 r C_0}{\phi K\alpha}[R_S^{C_0}-1].
\end{aligned}
\tag{6}
$$

In addition, assuming the S component, $S_i^\dagger$, and the corresponding C component, $C_i^\dagger$, are positive, then

$$C_i^\dagger = S_i^\dagger\left(B - \frac{re^{-\hat{d}\tau}}{r_0}\right) + \frac{\mu}{\phi}B, \quad with \quad B = \frac{r}{K\alpha}[S_0 - C_0],\ i = 1, 2 \tag{7}$$

$$E_i^\dagger = \left(\frac{\phi S_i^\dagger}{\phi S_i^\dagger + \mu}\right)\left(\frac{\alpha C_i^\dagger}{\hat{d}}[1 - e^{-\hat{d}\tau}]\right) \quad and \quad V_i^\dagger = \frac{\alpha C_i^\dagger}{\phi S_i^\dagger + \mu}. \tag{8}$$

Alternatively, provided that $\left(B - \frac{re^{-\hat{d}\tau}}{r_0} \neq 0\right)$, *each C component of* $\mathcal{E}_i$ *must satisfy the quadratic equation,*

$$P(C) = a_0C^2 + a_1C + a_2 = 0, \tag{9}$$

where

$$\begin{aligned}
a_0 &= \phi^2 r_0\left[r(\tilde{d} - \alpha e^{-\hat{d}\tau})\left(1 - \frac{\alpha(e^{-\hat{d}\tau} - 1)}{\hat{d}}\right) + r_0\left(\alpha - d(1 - \frac{\alpha(e^{-\hat{d}\tau} - 1)}{\hat{d}})\right)\right],\\
a_1 &= \frac{\phi}{\hat{d}}\left\{\left(\tilde{d}\mu r^2(\alpha - \hat{d} + \tilde{d}) + r\left[r_0\mu\left((d - \alpha)\hat{d} - d(\alpha + 2\tilde{d})\right) - 2\alpha\hat{d}\phi K\left(\tilde{d} - \frac{r_0}{2}\right)\right]\right.\right.\\
&\quad \left.\left. + r_0 d(K\alpha\hat{d}\phi + d\mu r_0)\right)e^{-\hat{d}\tau} + \alpha r\left[r\mu(\hat{d} - \tilde{d}) + K\alpha\hat{d}\phi + d\mu r_0\right]e^{-2\hat{d}\tau}\right.\\
&\quad \left. - \left[r_0\mu(d - \hat{d}) - \tilde{d}\mu r + K\hat{d}\phi(-r_0 + \tilde{d})\right](r_0 d - r\tilde{d})\right\},\\
a_2 &= \mu e^{-\hat{d}\tau}\left[\phi r^2\tilde{d}\left(\frac{\mu}{\phi} + S_0\right)\right](1 - \mathcal{R}_0).
\end{aligned} \tag{10}$$

by substituting S, which is a function of C, given in (7) in the polynomial (5).

Remark 1 When there are two interior (biologically relevant) equilibria, the one with the smaller C component will be designated as $\mathcal{E}_2^\dagger$, i.e., $C_2^\dagger < C_1^\dagger$. When there is only one interior equilibrium, then it will be referred to as $\mathcal{E}_1^\dagger$ or $\mathcal{E}^\dagger$.

Remark 2 By (7), it follows immediately that a necessary condition for the existence of a positive equilibrium is that $B > 0$, and this implies that $S_0 - C_0 = \frac{K}{rr_0}(r\tilde{d} - r_0 d) > 0$. This would be satisfied, for example, if the susceptible cells had the advantage of a faster replication rate and a lower death rate compared to the chronically infected cells.

Lemma 1 *Define* $\bar{r}_0 = \frac{r}{d}(\tilde{d} - \alpha e^{-\hat{d}\tau})$. *Then,* $\left(B - \frac{re^{-\hat{d}\tau}}{r_0}\right)|_{r_0=\bar{r}_0} = 0$. *If* $r_0 > \bar{r}_0$, *then* $B - \frac{re^{-\hat{d}\tau}}{r_0} < 0$ *and if* $r_0 < \bar{r}_0$, *then* $B - \frac{re^{-\hat{d}\tau}}{r_0} > 0$. *Furthermore,* $\bar{r}_0 < r_0^c$.

Proof Note that $B - \frac{re^{-\hat{d}\tau}}{r_0} = \frac{1}{r_0\alpha}(r(\tilde{d} - \alpha e^{-\hat{d}\tau}) - r_0 d) = \frac{d}{r_0\alpha}(\bar{r}_0 - r_0)$.

Also note that $r_0^c - \bar{r}_0 = \frac{\alpha\mu r^2 e^{\hat{d}\tau}}{d(\phi r S_0 + \mu r)} > 0$. □

Remark 3 We use Lemma 1, and both polynomials (5) and (9), where the constant coefficients are functions of $\mathcal{R}_S^{C_0}$, $\mathcal{R}_0$, respectively, in the proofs of Theorem 3, Theorem 4, and Theorem 5, since whenever $r_0 > \bar{r}_0$, we have $B - \frac{re^{-\hat{d}\tau}}{r_0} \neq 0$, and hence rearranging (7), $S^\dagger$ is well-defined as a function of $C^\dagger$.

In Theorems 1 and 2, we derived local stability conditions for $\mathcal{E}_0$, and $\mathcal{E}_c$. Notice that when both local stability conditions hold: $\mathcal{R}_0 < 1$ and $\mathcal{R}_S^{C_0} < 1$, the system (1) exhibits bistability with attractors $\mathcal{E}_c$ and $\mathcal{E}_0$. However, bistability can also occur with other types of attractors. We will also demonstrate that $\mathcal{E}_0$ can be stable at the same time as either $\mathcal{E}_1^\dagger$ or an orbitally asymptotically stable periodic solution.

In model (1), the parameters r_0 and α represent dual modes of viral replication. We will consider r_0 as a bifurcation parameter and investigate how the number and stability of the feasible boundary and interior equilibria change with respect to changes in r_0, as well as when there is bistability, i.e., when there are multiple local attractors.

In order to investigate how the dynamics change with respect to changes in r_0 and determine regions in parameter space where there is bistability, we consider the thresholds as functions of r_0 and solve $\mathcal{R}_0(r_0) = 1$ and $\mathcal{R}_S^{C_0}(r_0) = 1$, to determine values r_0^c and r_0^b, respectively. In particular,

$$\mathcal{R}_0(r_0^c) = 1 \Leftrightarrow r_0^c = \left(\tilde{d} - \frac{\phi S_0}{\phi S_0 + \mu}\alpha e^{-\hat{d}\tau}\right) / \left(1 - \frac{S_0}{K}\right). \tag{11}$$

and

$$\mathcal{R}_S^{C_0}(r_0^b) = 1 \Leftrightarrow r_0^b = \tilde{d}\left(1 - \frac{S_0}{K\left(1 + \frac{K\phi\alpha}{r\mu}\right)}\right)^{-1} = \frac{\tilde{d}(K\phi\alpha + r\mu)}{K\phi\alpha + d\mu}. \tag{12}$$

Remark 4 (i) The chronic infection reproduction number, $\mathcal{R}_0$, is an increasing function of r_0.

(ii) Since C_0 is an increasing function of r_0 and $C_0 > 0$ when $r_0 = \tilde{d}$, the susceptible invasion reproduction number, $\mathcal{R}_S^{C_0}(r_0)$ (defined in (4)) is a decreasing function of r_0 when $r_0 > \tilde{d}$. It has a vertical asymptote at $r_0 = \tilde{d}$, were $C_0 = 0$, and it is negative when $r_0 < \tilde{d}$. However, the corresponding singularity at $r_0 = \tilde{d}$ in $A_2(r_0)$ (defined in (6)) is removable (see Lemma 3(c) in Appendix).

The following theorem provides a condition for determining whether there is a *backward bifurcation* as r_0 increases through r_0^c. If so, if $r_0^c > 0$, for values of r_0 close to r_0^c, but $r_0 < r_0^c$, where $\mathcal{E}_0$ is therefore asymptotically stable, there would also be an unstable interior equilibrium close to $\mathcal{E}_0$.

Theorem 3 *System (1) has a backward bifurcation at $r_0 = r_0^c$ where $\mathcal{E}_0$ and $\mathcal{E}_1^\dagger$ coalesce, if $a_1(r_0^c) < 0$, where $a_1(r_0)$ is defined in (10) in Proposition (1), i.e., if the*

Table 1 Threshold Quantities

Reproduction numbers	Expression
Susceptible collapse	$\mathcal{R}_0^0 = \frac{r}{d}$
Chronic collapse	$\mathcal{R}_0^{C_0} = \frac{r_0}{\tilde{d}}$
Chronic infection	$\mathcal{R}_0 = \frac{r_0}{\tilde{d}}(1 - \frac{S_0}{K}) + \frac{\phi S_0}{\phi S_0 + \mu}\frac{\alpha}{\tilde{d}}e^{-\hat{d}\tau}$
Susceptible invasion	$\mathcal{R}_S^{C_0} = \frac{S_0}{C_0} - \frac{K\phi\alpha}{r\mu}$

Table 2 Equilibria & Local Stability

Equilibrium	Notation	S^*	E^*	C^*	V^*	Stability Condition
Susceptible collapse	$\mathcal{E}_0^0$	0	0	0	0	$\mathcal{R}_0^0 < 1$
Infection free	$\mathcal{E}_0$	S_0	0	0	0	$\mathcal{R}_0 < 1$
Chronic only	$\mathcal{E}_c$	0	0	C_0	V_c	$\mathcal{R}_S^{C_0} < 1$
Interior	$\mathcal{E}_i^\dagger, i = 1, 2$ (*),(**)	$S_i^\dagger$	$E_i^\dagger$	$C_i^\dagger$	$V_i^\dagger$	***

(*) When two interior equilibria are biologically relevant, we denote by $\mathcal{E}_1^\dagger$, the one with the larger C component, i.e., $C_1^\dagger > C_2^\dagger$ (with the corresponding changes in the other components). (See *Proposition* 1 and Fig. 1b).
(**) $\mathcal{E}_1$ can undergo *Hopf bifurcation* (See *Remark* 8).
(***) The analysis in conjunction with the bifurcation diagrams seem to indicate that when it exists, $\mathcal{E}_2^\dagger$ is always unstable. Also when it exists, stability of $\mathcal{E}_1^\dagger$ depends on whether or not it has undergone a Hopf bifurcation)

following expression is negative:

$$e^{-\hat{d}\tau}\left(\alpha\hat{d}r^2\phi^2S_0^2 + d\hat{d}\mu^2r^2 + rK\mu\phi\left\{r[\hat{d}(d+\alpha) + \alpha d] - d^2(\alpha+\hat{d})\right\}\right)$$
$$-r^2d\mu\phi\alpha S_0e^{-2\hat{d}\tau} - r^2\hat{d}\tilde{d}(\phi S_0 + \mu)^2 \tag{13}$$

and a forward bifurcation if it is positive, i.e., $a_1(r_0^c) > 0$.

The proof is in Appendix A.4.

Remark 5 In the case of backward bifurcation at the point r_0^c, we have observed the following dynamics of the system near $r_0 < r_0^c$:

i) $\mathcal{E}_0$, is the only stable invariant set, and $\mathcal{E}_i$, $i = 1, 2$ both exist, but are unstable. This can occur, for example, if there is a homoclinic bifurcation resulting in the disappearance of the periodic solution (see Fig. 7).
ii) bistability:

– $\mathcal{E}_0$ and $\mathcal{E}_c$ are both stable and there is a unique unstable interior equilibrium, $\mathcal{E}^\dagger$, or

- $\mathcal{E}_0$, and $\mathcal{E}_1^\dagger$ are both stable, and $\mathcal{E}_2$ is unstable, (for an example, see Fig. 1b), where the bistability involves two stable equilibria that occur to the left of the first Hopf bifurcation, near the saddle-node bifurcation), or
- a limit cycle and $\mathcal{E}_0$ are both stable, $\mathcal{E}_c$ exists and is unstable, and $\mathcal{E}_i$, $i = 1, 2$ both exist and are unstable (for an example, see Fig. 1b).

In the following result (proved in Appendix A.5), we show that a forward or a backward bifurcation can also occur when r_0 increases through r_0^b (defined in (12)). Note that r_0^b is always positive, since $0 < 1 - \frac{S_0}{K} < 1 - \frac{S_0}{K}\left(1 + \frac{K\phi\alpha}{r\mu}\right)^{-1}$.

Remark 6 When $r_0 = r_0^b$, i.e., $\mathcal{R}_S^{C_0}(r_0) = 1$, there is a transcritical bifurcation involving $\mathcal{E}_c$, the chronic only (susceptible free) equilibrium and the interior equilibrium, $\mathcal{E}_1$. As r_0 increases through r_0^b, branches of these equilibria cross and exchange stability. We distinguish between a forward and a backward transcritical bifurcation in this case, by retaining the key features of the more familiar meaning of forward and backward transcritical bifurcation used in epidemiology where it is used to describe a transcritical bifurcation between the disease free equilibrium and an endemic equilibrium instead of a susceptible free equilibrium and one with positive amounts of virus. In the more familiar case, backward bifurcation refers to the existence of the endemic equilibrium when the reproduction number is less than one. When it first appears it is unstable and there is usually an associated saddle-node bifurcation of the endemic equilibrium resulting in bistability near the transcritical bifurcation on the side where the reproduction number is less than one. This is the interpretation in Theorem 3, when $r_0 = r_0^c$. When instead, $r_0 = r_0^b$, we let $\mathcal{E}_c$, the susceptible free equilibrium, play the role of the disease free equilibrium and $\mathcal{E}_1$ play the role of the endemic equilibrium, (although the C and V components are positive in both of these equilibria and so they both could be considered endemic equilibria).

We call this transcritical bifurcation at r_0^b a backward bifurcation if $S^\dagger$ is an increasing function of r_0 at r_0^b and a forward bifurcation if it is a decreasing function of r_0. In the case of the backward bifurcation, when $r_0 < r_0^b$, (i.e., $R_S^{C_0} > 1$), $S^\dagger < 0$, and hence $\mathcal{E}_1^\dagger$ does not exist close to $\mathcal{E}_c$, and $\mathcal{E}_c$ is unstable. On the other side of the bifurcation, where $r_0 > r_0^b$, (i.e., $R_S^{C_0} < 1$), $\mathcal{E}_1^\dagger$ exists and is unstable, close to $\mathcal{E}_c$, and $\mathcal{E}_c$ is locally asymptotically stable. A saddle-node bifurcation for $r_0 > r_0^b$ is expected resulting in the existence of a stable $\mathcal{E}_2^\dagger$ and hence bistability. In the case of a forward bifurcation, when $r_0 < r_0^b$, (i.e., $R_S^{C_0} > 1$), $\mathcal{E}_1^\dagger$ exists and is locally asymptotically stable close to $\mathcal{E}_c$, and $\mathcal{E}_c$ is unstable. On the other side of the bifurcation, where $r_0 > r_0^b$, (i.e., $R_S^{C_0} < 1$), $\mathcal{E}_1^\dagger$ does not exist close to $\mathcal{E}_c$, and $\mathcal{E}_c$ is locally asymptotically stable. An example of a forward bifurcation at r_0^b and a backward bifurcation at r_0^c is illustrated in Fig. 1b). An example of a backward bifurcation at r_0^b and a forward bifurcation at r_0^c is illustrated in Fig. 2.

Theorem 4 *System (1) has a backward bifurcation at $r_0 = r_0^b$, where $\mathcal{E}_1^\dagger$ and $\mathcal{E}_c$ coalesce, if $A_1(r_0^b) > 0$, where $A_1(r_0)$ is defined in (30), i.e., if the following expression*

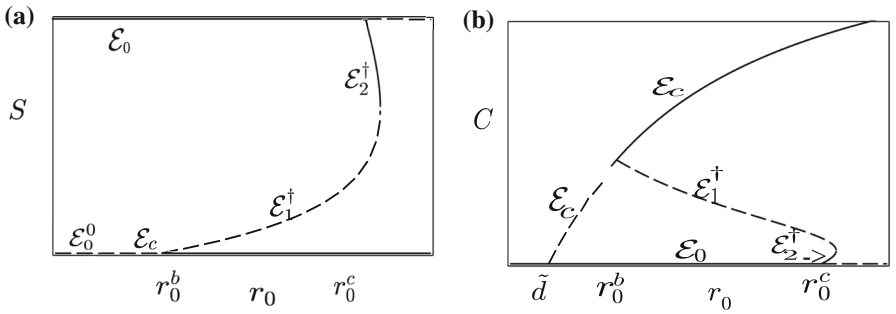

Fig. 2 One-parameter bifurcation diagrams, **a** showing the S component and **b** the C component of the equilibria as r_0 varies, illustrating a forward bifurcation at $r_0 = r_0^c$ involving $\mathcal{E}_0$ and $\mathcal{E}_2^\dagger$ and a backward bifurcation at r_0^b involving $\mathcal{E}_c$ and $\mathcal{E}_1^\dagger$, as described in Theorems 3 and 4. The graphs also demonstrate the different cases described in Theorem 5, and in particular, that whenever there is a forward bifurcation at r_0^c and a backward bifurcation at r_0^b, the system displays bistability for some values of r_0 with $\mathcal{R}_0 > 1$ (i.e., $r_0 > r_0^c$), as is indicated as one of the possibilities in Theorem 5(b). The parameter values are: $K = 10^7$, $\alpha = 0.1$, $r = 0.1$, $\tau = 320$, $d = 0.015625$, $\tilde{d} = 0.01328$, $\hat{d} = 0.0065$, $\phi = 10^{-8}$, $\mu = 0.1$, resulting in $S_0 = 16,875,000$, $r_0^b = 0.01848$, and $r_0^c = 0.03477$

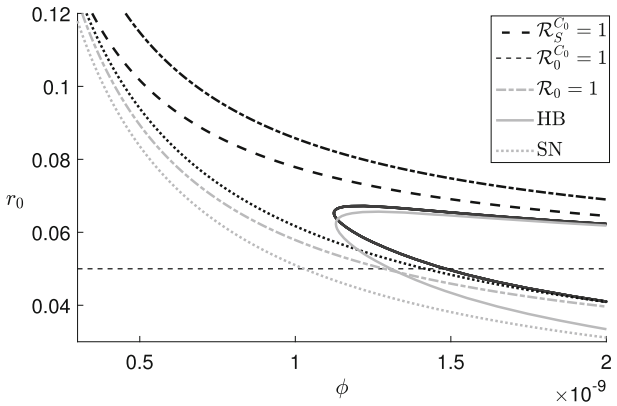

Fig. 3 Two-parameter bifurcation diagram with bifurcation parameters r_0 and ϕ showing how time delay affects the bifurcation curves. The light grey curves are for $\tau = 0$, i.e., the case of no delay. The black curves are for $\tau = 2$. However, the dashed black curves for $\mathcal{R}_0^{C_0} = 1$ and $\mathcal{R}_S^{C_0} = 1$ are the same for both values of the delay, and so the grey curve and the black curve overlap and only the black dashed curves show up. Increasing the delay moves the saddle-node (SN) curve and the curve $\mathcal{R}_0 = 1$ upwards (with increasing bistable parameter region) and the Hopf bifurcation (HB) bifurcation curve up and slightly to the left (with decreasing the parameter region bounded by Hopf bifurcation points)

is positive:

$$\begin{aligned}&(-d\hat{d}\mu^2 r - K\phi\alpha\mu(\hat{d}(d+r) + \tilde{d}(r-d)) - (K\phi\alpha)^2\hat{d})e^{-\hat{d}\tau}\\&-\mu\tilde{d}(-\hat{d}\mu r + K\phi((d-r-\hat{d})\alpha + \hat{d}(d-r)))\end{aligned} \tag{14}$$

and a forward bifurcation if it is negative, i.e., $A_1(r_0^b) < 0$.

The proof is in Appendix A.5.

Given that r_0^c and r_0^b are the critical values of the bifurcation parameter r_0 such that $\mathcal{R}_0(r_0^c) = 1$, and $\mathcal{R}_S^{C_0}(r_0^b) = 1$, respectively, we next investigate how the number of interior equilibria change as r_0 varies, and show how this depends on the relative values of r_0, r_0^c, and r_0^b.

Theorem 5 *Consider system (1).*

(a) *If* $r_0 \in (\max\{0, r_0^c\}, r_0^b)$, *then there is a unique interior equilibrium.*
(b) *If* $r_0 > \max\{r_0^c, r_0^b\}$, *then there are no interior equilibria, unless* $A_0(r_0) \leq 0$ *and* $r_0 \in (\max\{r_0^c, r_0^b\}, r_0^*)$, *where* $r_0^* = \frac{r\tilde{d}}{d}$. *In that case, if* $A_0(r_0) < 0$, *then there are at most 2 interior equilibria and if* $A_0(r_0) = 0$, *but* $A_0(r_0)$ *is not identically zero, then there is at most one interior equilibrium.*
(c) *If* $r_0^b < r_0 < r_0^c$, *then there is a unique interior equilibrium.*
In addition, $\mathcal{E}_0$ *is locally asymptotically stable and* $\mathcal{E}_c$ *exists and is also locally asymptotically stable (i.e., there is bistability with the two attractors,* $\mathcal{E}_0$ *and* $\mathcal{E}_c$*).*
(d) *If* $0 < r_0 < \min\{r_0^c, r_0^b\}$,
then

i) if $A_0(r_0) > 0$, *where the expression for* A_0 *is given in (6), there are at most 2 interior equilibria, and*
ii) if $A_0(r_0) \leq 0$, *then there are no interior equilibria.*

The proof is in Appendix A.6.

Remark 7 See Figs. 1b and 2a, b for an illustration of the cases described in Theorem 5 and for examples of the forward and backward bifurcations described in Theorems 3 and 4.

Remark 8 In the special case of our system when there is no delay and no vertical transmission (i.e., $\tau = 0, r_0 = 0$), model (1) can be scaled to a system given in Beretta and Kuang (1998). Therefore, in that special case, the stability result and the Hopf bifurcation conditions for that system in Beretta and Kuang (1998) apply to our system. Hence, we can immediately conclude that our system can have Hopf bifurcations. However, without any of these simplifications, we do not attempt to investigate the characteristic equation, since it is a transcendental equation with very complicated expressions for its coefficients. Instead, in Sect. 4, we use a numerical approach to determine the effect of delay time, τ, on the infection dynamics by varying certain important parameters.

So far we have been concerned with getting the global picture of the model dynamics via investigating a number of equilibrium points and their local stability properties along with bifurcation analysis. However, often times, this is not enough to capture all the possible outcomes of the model. For example, as Jansen and Sigmund mention in their paper (Jansen and Sigmund 1998), "Environmental perturbations are often vigorous shake-ups, rather than gentle stirrings. Furthermore, there may be no stable equilibrium to return to, but rather a periodic or chaotic attractor". In this regard, our next result (with proof based on an idea developed in Salceanu (2011) or Salceanu

and Smith (2009)) is concerned with the *global* dynamics of the model. Namely, we establish conditions for different categories of the cell population (susceptible, chronically infected, or both) to recover from these "vigorous shake-ups" and survive in the long term (not necessarily at an equilibium point), with densities about a certain positive threshold. Moreover, this threshold remains unchanged with small variations in the factors that determine the interactions among the cells (that is, the parameters involved in the model). From a mathematical viewpoint, this is addressed through the concept of *robust uniform persistence*, the clear meaning of which will be stated in the next theorem.

Let $\Gamma \subset \mathbb{R}^6_+$ be a bounded set of parameters for (1) and fix $\gamma_0 \in \Gamma$. Let "$||\cdot||$" denote the Euclidean norm.

Theorem 6 (robust uniform persistence) *The following hold.*

i) There exist $\varepsilon, \delta > 0$ *such that* $\liminf_{t\to\infty} S(t) + C(t) > \varepsilon$, *for all solutions of (1) with initial conditions* $\Phi \in \mathcal{D}$ *satisfying* $\Phi_1(0) + \Phi_3(0) > 0$, *corresponding to all* $\gamma \in \Gamma$ *with* $||\gamma - \gamma_0|| < \delta$.

ii) If $R_S^{C_0} > 1$, *then there exists* $\varepsilon, \delta > 0$ *such that* $\liminf_{t\to\infty} S(t) > \varepsilon$, *for all solutions of (1) with initial conditions* $\Phi \in \mathcal{D}$ *satisfying* $\Phi_1(0) > 0$, *corresponding to all* $\gamma \in \Gamma$ *with* $||\gamma - \gamma_0|| < \delta$.

iii) If $\mathcal{R}_0 > 1$, *then there exist* $\varepsilon, \delta > 0$ *such that* $\liminf_{t\to\infty} \min\{C(t), V(t)\} > \varepsilon$, *for all solutions of (1) with initial conditions* $\Phi \in \mathcal{D}$ *satisfying* $\sup_{t\in[-\tau,0]} ||(\Phi_3(t), \Phi_4(t))|| > 0$, *corresponding to all* $\gamma \in \Gamma$ *with* $||\gamma - \gamma_0|| < \delta$.

iv) If $\mathcal{R}_0 > 1$ *and* $\mathcal{R}_S^{C_0} > 1$, *then there exists* $\varepsilon, \delta > 0$ *such that* $\liminf_{t\to\infty} \min\{S(t), C(t), V(t)\} > \varepsilon$, *for all solutions of (1) with initial conditions* $\phi \in \mathcal{D}$ *satisfying* $\Phi_1(0) \sup_{t\in[-\tau,0]} ||(\Phi_3(t), \Phi_4(t))|| > 0$, *corresponding to all* $\gamma \in \Gamma$ *with* $||\gamma - \gamma_0|| < \delta$.

The proof is in Appendix A.7.

4 Bifurcation diagrams & numerical simulations

In this section, we use one- and two-parameter bifurcation diagrams obtained numerically using the Matlab [33] toolbox, DDE-Biftool (Engelborghs et al. 2002, 2001) to demonstrate how the dynamics of the model depend on the choice of parameters. DDE-Biftool is a package specifically created to do numerical bifurcation analysis and stability analysis of systems of delay differential equations. It uses continuation algorithms that identify and follow both stable and unstable equilibria and periodic solutions as one or two parameters are varied. In particular, we focus on how the range of possible dynamics of the model, in different regions in parameter space, depends on four parameters: the time delay, τ; the infected cell net growth rate, r_0; the infection rate, ϕ; and the chronic cell replication rate, α. In all of the one-parameter bifurcation diagrams, solid curves indicate the value of the component on the vertical axis of stable equilibria, dashed curves the value of the component of the unstable equilibria, and filled circles the largest and smallest values of the component on an orbitally asymptotically stable periodic solution. (We did not find any unstable periodic solutions in this

Table 3 Estimated parameter values from phage-microbe systems for the model (1)

Parameter (Susceptible)	Value	Source	Unit	Parameter (Eclipse)	Value	Source	Unit
r	0.339	Gulbudak and Weitz (2016)	hrs^{-1}	$\hat{d}$	1/24	see text	hrs^{-1}
K	8.947×10^8	Gulbudak and Weitz (2016, 2019)	Cells/ml	τ	1/6	See text	hrs
d	1/24	Gulbudak and Weitz (2016)	hrs^{-1}				
Parameter (Chronic)	Value	Source	Unit	Parameter (Chronic)	Value	Source	Unit
r_0	0.2	Gulbudak and Weitz (2016, 2019)	hrs^{-1}	$\tilde{d}$	1/20	Gulbudak and Weitz (2016, 2019)	hrs^{-1}
ϕ	0.2×10^{-10}	Gulbudak and Weitz (2016)	ml/hr	μ	0.0866	Gulbudak and Weitz (2016)	hrs^{-1}
α	1/21	See text					

Table 4 Invariant Sets of System (1) in Regions $I - IX$ in Fig. 1

Region	Stable invariant sets	Unstable invariant sets
I	$\mathcal{E}_0,\ \mathcal{E}_1^\dagger$	$\mathcal{E}_0^0,\ \mathcal{E}_2^\dagger$
II	$\mathcal{E}_0,$ periodic solution*	$\mathcal{E}_0^0,\ \mathcal{E}_c,\ \mathcal{E}_i^\dagger, i = 1, 2$
III	$\mathcal{E}_0,\ \mathcal{E}_1^\dagger$	$\mathcal{E}_0^0,\ \mathcal{E}_c,\ \mathcal{E}_2^\dagger$
IV	$\mathcal{E}_0,$ periodic solution*	$\mathcal{E}_0^0,\ ,\ \mathcal{E}_i^\dagger, i = 1, 2$
V	periodic solution	$\mathcal{E}_0^0,\ \mathcal{E}_0,\ \mathcal{E}_c,\ \mathcal{E}_1^\dagger$
VI	$\mathcal{E}_0$	$\mathcal{E}_0^0$
VII	$\mathcal{E}_0$	$\mathcal{E}_0^0,\ \mathcal{E}_c$
$VIII$	$\mathcal{E}_1^\dagger$	$\mathcal{E}_0^0,\ \mathcal{E}_0,\ \mathcal{E}_c$
IX	$\mathcal{E}_c$	$\mathcal{E}_0^0,\ \mathcal{E}_0$

(*) It is possible that there is a curve of homoclinic bifurcations in these regions that causes the periodic solution to disappear. See Figs. 4 and 5 for more details

system.) The timeseries simulations were done using XPPAUT (Ermentrout 2002). Unless, otherwise stated, we use parameter values for phage-microbe systems estimated from the literature in our bifurcation diagrams and simulations, with citations to the sources, given in Table 3.

Here, we demonstrate *(i) the different types of bifurcations that system* (1) *can exhibit.* Next, we investigate (ii) *how the time delay, τ, in eclipse stage reshape these regions.* By using (i) and (ii), in the next section, we investigate *how increasing the time delay affects the fate of temperate viruses and their hosts in phage-microbe systems and in within-host persistent infections.*

An experimental study done on filamentous (chronically infecting) phages suggest that the eclipse stage usually takes 12 minutes after induction at time $t = 0$ (Ploss and Kuhn 2010); therefore $\tau = 1/6$ hours. However when we do not use the time delay as a bifurcation parameter, we fix the time delay to be $\tau = 0$, 1, or $\tau = 2$ to show range of distinct population dynamic outcomes. In addition, the same study shows that by the secretory process, for the system considered, each cell budded off, on average, 6 viral particles per minute. Therefore, the budding rate is fixed to be $\alpha = 1/10$ viruses per hour per cell in the prior study (Gulbudak and Weitz 2019). Since this value depends on the actual biological system we consider, to present the distinct rich bifurcation dynamics displayed by our system, we use $\alpha = 1/21$, when r_0, ϕ, and τ are used as bifurcation parameters. We assume that temperate infection does not harm the cellular hosts and so we take $\hat{d} = d = 1/24$.

In Fig. 1a, we provide a two-parameter bifurcation diagram that illustrates the sensitivity of the dynamics of model (1) to two of the parameters: the infection rate, ϕ, versus the net infected cell growth rate (vertical transmission), r_0, when $\tau = 1$. In Fig. 3, the analogous two-parameter bifurcation diagrams with $\tau = 0$ and $\tau = 2$ are superimposed to help understand the effect of different time delays on these curves, and hence on the dynamics. In particular, we graph the two-parameter bifurcation curves of the three transcritical bifurcations. One curve shows the curve $\mathcal{R}_0 = 1$

as a function of r_0. This is where the branches of the equilibria $\mathcal{E}_0$ and $\mathcal{E}_2^\dagger$ cross as r_0 varies. Another curve shows the curve $\mathcal{R}_S^{C_0} = 1$ as a function of r_0. This is where the branches of $\mathcal{E}_c$ and $\mathcal{E}_1^\dagger$ cross as r_0 is varied. A third curve shows the curve $\mathcal{R}_0^{C_0} = 1$ as a function of r_0. This is where the branch of $\mathcal{E}_c$ and of $\mathcal{E}_0^0$ cross as r_0 varies (i.e., where $r_0 = \tilde{d}$). To actually see these curves cross, see the corresponding one-parameter diagram in Fig. 1b. (Note, that if when they cross, on one side of the curve the equilibrium is no longer biologically relevant, since one of the components of the corresponding equilibrium is negative, that part of the curve is not shown.) We also plot the curve of saddle-node bifurcations (SN) of the interior equilibrium, where the two curves of interior equilibria meet) and the curve of Hopf bifurcations (HB) of $\mathcal{E}_1^\dagger$, where a family of periodic solutions is either born or disappears. These five curves divide (ϕ, r_0) parameter space into nine regions, each having the different dynamics listed in Table 4. For parameters in the regions labelled (I) and (III) there are two attracting invariant sets, the infection free equilibrium, $\mathcal{E}_0$ and $\mathcal{E}_1^\dagger$, i.e., this is a region of bistability. In regions (II) and (IV), either these two sets are attracting or $\mathcal{E}_0$ and an orbitally asymptotically periodic solution, born from the Hopf bifurcation of $\mathcal{E}_1^\dagger$, when it destabilizes, are attracting. However, as in the case for $\tau = 2$, that will be explained later in Figs. 4 and 5, for a larger value of ϕ than shown, the saddle-node curve and Hopf bifurcation curve might meet at a Bogdanov–Takens bifurcation and so there could possibly be a curve of homoclinic bifurcations emanating from the intersection point. This would result in the disappearance and then reappearance of a periodic solution as r_0 increases through two homoclinic bifurcations. This curve would therefore provide a border for subregions of regions II and IV where only $\mathcal{E}_0$ is attracting.

If in Fig. 1a, we fix $\phi = 1.6 \times 10^{-9}$, shown as the vertical dotted red line, and only allow r_0 to vary along this line, one obtains the corresponding one-parameter bifurcation diagram shown in Fig. 1b. As r_0 increases, the dynamics change as the system moves from one region in parameter space to another by undergoing the following sequence of bifurcations:

$$VI \overset{(\mathrm{SN})}{\rightarrow} I \overset{(\mathrm{HB})}{\rightarrow} IV \overset{(\mathcal{R}_0^{C_0}=1)}{\rightarrow} II \overset{(\mathcal{R}_0=1)}{\rightarrow} V \overset{(\mathrm{HB})}{\rightarrow} VIII \overset{(\mathcal{R}_S^{C_0}=1)}{\rightarrow} IX.$$

See Table 4 to see which invariant set either appears or disappears and how their stability changes as r_0 increases along this line. We can see that for this sequence of bifurcations, there is an orbitally asymptotically stable periodic solution in regions II, IV, and V, and bistability in regions I, II, and IV. If instead, we were to fix $\phi = 1 \times 10^{-9}$, in Fig. 1a, i.e., to the left of the curve of Hopf bifurcations, and let r_0 vary, the corresponding sequence of bifurcations would be

$$VI \overset{(\mathcal{R}_0^{C_0}=1)}{\rightarrow} VII \overset{(\mathrm{SN})}{\rightarrow} VIII \overset{(\mathcal{R}_0=1)}{\rightarrow} VIII \overset{(\mathcal{R}_S^{C_0}=1)}{\rightarrow} IX.$$

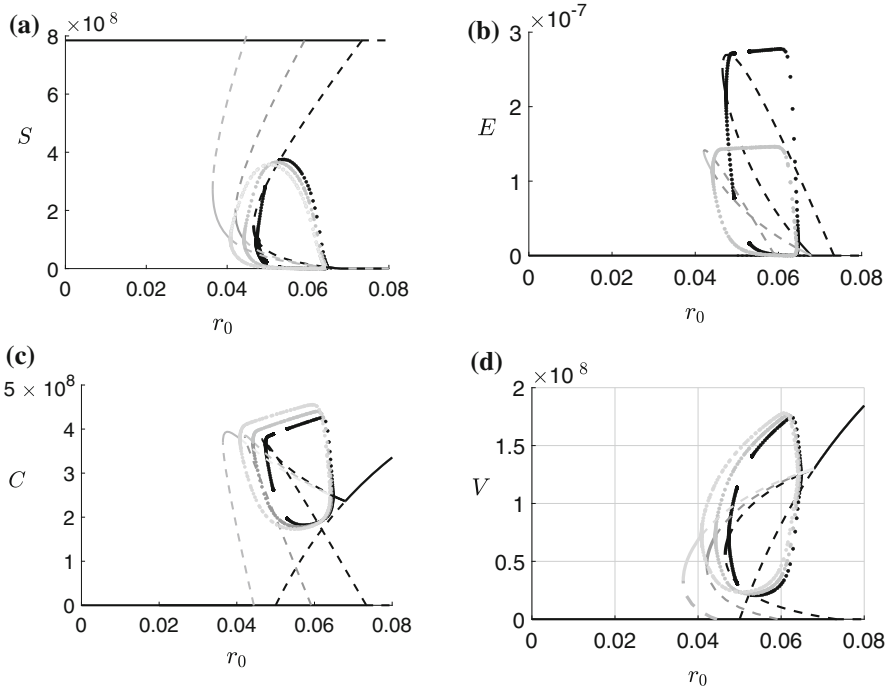

Fig. 4 Superimposed, one-parameter bifurcation diagrams with r_0 as the bifurcation parameter, to compare the impact of the eclipse stage time delay on the infection dynamics for $\tau = 0$, 1, and 2. In all four graphs, the parameter values used, apart from the bifurcation parameter, r_0, are given in Table 3, except $\alpha = 1/21$ and $\phi = 1.6 \times 10^{-9}$, as in Fig. 1b. In all the graphs **a**–**d** the bifurcation diagram for $\tau = 0$ (no delay) is the lightest grey, $\tau = 1$, medium gray, and $\tau = 2$, black. However, the curve corresponding to the component of $\mathcal{E}_c$, is independent of τ, and so all those curves overlap, and hence only appear in black. Note that when $\tau = 0$, there is no eclipse phase, and hence in **b** there are only two superimposed bifurcation diagrams

Note that from Fig. 1a, we can similarly determine the different sequences of bifurcations that are possible if we fix r_0 and allow ϕ to vary, so that we move from one region to the next.

Figures.1(b) and 2 illustrate different cases of forward and backward bifurcations at r_0^c and at r_0^b described in Theorems 3 and 4. Fig. 1(b) shows that whenever there is a backward bifurcation at r_0^c and a forward bifurcation at r_0^b, there is bistability for some values of $r_0 < r_0^c$ and Fig. 2 shows that if there is a forward bifurcation at r_0^c and a backward bifurcation at r_0^b, that there are values of $r_0 > r_0^c$ where there is bistability. This case is particularly interesting, since in this case $\mathcal{R}_0 > 1$. These two figures also demonstrate how the number of interior equilibria depends on the relative values of r_0^c and r_0^b as described in Theorem 5.

To investigate the impact of the length of the time delay in the eclipse stage on the dynamics as r_0 varies, in Fig 3 we display super-imposed, two-paramter bifurcation diagrams for delay times $\tau = 0$ and 2 and in Fig. 4 we display, superimposed, one-parameter bifurcation diagrams for delay times $\tau = 0, 1, 2$. Observe that as the delay time increases, the interval of values of r_0 between the saddle-node bifurcation (where

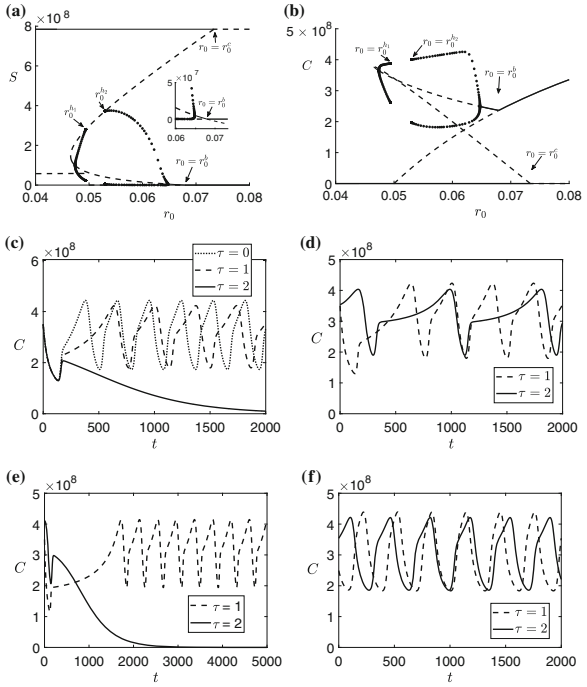

Fig. 5 **a–b** The one-parameter bifurcation diagrams in Fig. 4a, c, respectively, for $\tau = 2$. All parameters are also the same as in Fig. 1b except $\tau = 2$ instead of $\tau = 1$. These one-parameter bifurcation diagrams illustrate a backward bifurcation at $r_0 = r_0^c$ and a forward bifurcation at $r_0 = r_0^b \approx 0.068$, in agreement with the hypotheses of Theorems 3 and 4. For r_0 between the saddle-node bifurcation of the interior equilibrium at $r_0 \approx 0.465$ and $r_0^c \approx 0.073$, there is bistability, except in the gap between $r_0^{h1} \approx 0.049$ and $r_0^{h2} \approx 0.053$. c)-f) Corresponding timeseries providing evidence of two suspected homoclinic bifurcations, at $r_0 = r_0^{h1}$ and $r_0 = r_0^{h2}$. The bifurcation diagrams in a) and b) have a gap in the curve of periodic solutions. As r_0 increases, the periodic solution disappears at r_0^{h1} and then reappears at r_0^{h2} due to the suspected homoclinic bifurcations. We focus on the homoclinic bifurcation for the larger value of r_0 that occurs at $r_0^{h2} \approx 0.053$. In d) $r_0 = 0.054$, close to but to the right of r_0^{h2}. In e) $r_0 = 0.051$, a value of r_0 in the gap between the suspected homoclinic bifurcations. In f) $r_0 = 0.06$, to the right of r_0^{h2} and farther away than the graph in e). We use the same (referred to as common) initial data for all of the solutions: $S(t) = 1000$, $E(t) = 100$, $C(t) = 3.5 \times 10^8$, $V(t) = 1000$ for $t \in [-\tau, 0]$, except for the solutions for $\tau = 2$ in (e) and (f). In c) for r_0 close to but to the right of r_0^{h2}, there is bistability. Using the common initial data, the solutions converge to a periodic solution for $\tau = 0$ and $\tau = 1$, but the C component of the solution for $\tau = 2$ converges to 0, i.e., the solution converges to $\mathcal{E}_0$ as predicted by the bifurcation diagrams in a)-b). To obtain the obtain the periodic solution in d) for $\tau = 2$, we iterated the solution for $\tau = 1$ for 2000 steps to converge to the periodic solution and used the end of that solution as initial data to obtain the periodic solution for $\tau = 2$, thus illustrating the bistability. In e), in the gap, we iterated the solution for $\tau = 1$ for 5000 steps to converge to the periodic solution and using the end of that solution as initial data, the C component still converged to 0, providing evidence that there is no stable periodic solution when $\tau = 2$ and r_0 is in the gap. f) When $r_0 = 0.06$ for both $\tau = 1$ and $\tau = 2$, i.e., further from the suspected homoclinic bifurcation, using the common initial data, notice that although the period for $\tau = 2$ is larger than for $\tau = 1$, there is a much larger increase in the period for $\tau = 2$ in d) where r_0 is closer to the suspected homoclinic bifurcation, a hallmark of a homoclinic bifurcation. A similar scenario can be shown near the suspected homoclinic bifurcation at r_0^{h1}

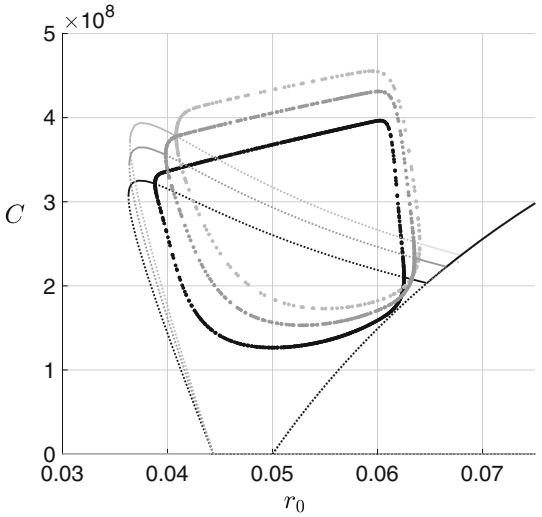

Fig. 6 One-parameter bifurcation diagrams with r_0 as the bifurcation parameter, to compare the impact of the time delay in the eclipse stage on the infection dynamics when $\tau = 0$ (lightest grey), $\tau = 1$ (medium grey) and $\tau = 5$ (black). The parameter values are the same as the ones used in Fig. 4, except α is replaced by $\frac{\alpha}{e^{-d\tau}}$, in order to compare the impact of the time delay in the eclipse stage on infection dynamics when the effect of the time delay in the eclipse stage is compensated for by increasing the burst size, as suggested in Abedon et al. (2001). By replacing α by $\frac{\alpha}{e^{-d\tau}}$, r_0^c is the same for all three time delays, i.e., the backward bifurcation at $r_0 = r_0^c$ occurs for the same value of r_0. The graph shows that the interval of r_0 values where there is bistability involving a periodic solution is larger for larger values of τ, since the leftmost Hopf bifurcation occurs at a smaller value of r_0 for larger values of the delay, but the interval where there is persistence is smaller, since r_0^b is smaller for larger values of the delay. However, the interval for which chronic infected cells survive is almost the same, since the saddle-node bifurcation occurs at almost the same value of r_0

the two interior equilibria suddenly appear) and the transcritical bifurcation (where $r_0 = r_0^c$ and $\mathcal{E}_2^\dagger$ disappears) gets larger, even though the saddle-node bifurcation moves to the right as τ increases. For both $\tau = 0$ and $\tau = 1$, there is bistability in this interval. However, for $\tau = 2$ there appear to be two homoclinic bifurcations (see the gap in the black curve of periodic solutions).

In Fig. 5 a) and b), we reproduce the graphs shown in Fig. 4 a) and c), respectively, for $\tau = 2$, in order to provide evidence for two suspected homoclinic bifurcations at $r_0^{h_1}$ and $r_0^{h_2}$. As r_0 increases through the first suspected homoclinic bifurcation at $r_0^{h_1}$, (the beginning of the gap in the Hopf bifurcation curve), the attracting periodic solution disappears and only $\mathcal{E}_0$ is attracting. As r_0 increases further, there appears to be a second homoclinic bifurcation at $r_0 = r_0^{h_2}$, where the periodic solution reappears as r_0 increases past $r_0^{h_2}$.

Using timeseries in e) we investigate the dynamics in the gap. As indicated in the bifurcation diagrams a)-b), there does not appear to be a stable periodic orbit in the gap when $\tau = 2$ as there is when $\tau = 0$ and $\tau = 1$. In c) and d) close to, but to the right of $r_0^{h_2}$ the same initial data is used for all three solutions. The graphs in c), d) and f) are for r_0 to the right of $r_0^{h_2}$ with the graphs in c) and d) for a value of r_0 closer to

$r_0^{h_2}$ than in f). While the period of both solutions in d) are larger than in f), the period of the solution for $\tau = 2$ is significantly larger in d) than in f) showing that as r_0 gets closer to $r_0^{h_2}$, the period of the solution for $\tau = 2$ increases significantly, a hallmark of a homoclinic bifurcation. A similar procedure can be done to the left of $r_0^{h_1}$, showing evidence for a homoclinic bifurcation there as well.

5 Biological implications and importance of bifurcations

A major goal of our paper is to analytically prove the occurrence of the different bifurcations, which do have biological and dynamical relevance such as bistability. The analytical results pave the way for our understanding of the complex dynamics and guide/verify our numerical exploration. Every time the system undergoes a bifurcation as a parameter is varied, the population dynamics changes. In particular, there is a change in the number and/or stability of the attractors. In a prior work, for the same model without delay, we show how the population dynamics changes as the bifurcation parameter r_0 increases (see Fig. E4 in Gulbudak and Weitz (2019)). Here, we add to the understanding of chronically infecting virus dynamics by employing a deeper bifurcation analysis in the more complex and biologically detailed delay model. In particular, we provide extensive analytical and numerical results on bifurcations and the impact of the delay on the dynamics. The specific formulae for bifurcations in terms of the model parameters, such as Theorems 3, 4 and 5, guarantee the existence of bifurcations, and two-parameter bifurcation diagrams show different regions in parameter space separated by the bifurcation curves.

When systems display bistable dynamics, outcomes of evolving population dynamics depend on initial population density. In this case, when estimated parameter values are in the bistable parameter region environmental fluctuations or disturbances that impulsively change the population density, resetting the initial conditions, might lead to the state of the system moving to the basin of attraction of another attractor. In this case, the population dynamics would follow a different trajectory. This might be detrimental or beneficial to the host cells and the virus population. Some of the examples can be seen in Gulbudak and Martcheva (2013) in the context of disease models, where by using temporary control measures (playing the role of disturbances), one can push the solutions into the basin of attraction of the disease-free equilibrium (when there is backward bifurcation) or the interior equilibrium where the infected population component is small (for the *forward hysteresis* case (Gulbudak and Martcheva 2013)) for a favorable disease control outcome. In our case, in Fig. 5 we observe that with only a slight change in the initial condition (see solid curves in Fig. 5 c)-d) for the case $\tau = 2$), the infected cell population either persists, displaying oscillatory dynamics, or dies out. For example, in the context of tumor oncolytic virotherapy, when $\mathcal{R}_0 < 1$, higher initial virus and infected tumor density can push infected tumor density solutions into the basin of attraction of the interior equilibrium (or of limit cycles) with the optimal amount of infected tumors density, leading to a better treatment outcome. Here a better treatment outcome might be that the infected cells are recognized by the immune response and/or the virus establishes infection throughout the tumor cells.

Therefore, choosing a virus strain with larger eclipse stage duration, τ, and increasing virus inoculum (initial virus concentration given to patients) might increase the chance of successful treatment (see solid curves in Fig. 5 c)-d)).

For HIV, larger delay in the eclipse stage can be detrimental to virus survival, in particular, when immune response targets infected cells in the eclipse stage, as recent studies suggest (Buckheit et al. 2013). On the other hand, HIV benefits from latently infected cells during antiviral treatment, and possibly during initial infection, where an increased delay in viral production can promote persistence (Rouzine et al. 2015). In Fig. 5c), we observe that despite the same initial data used for all three values of τ, in the case of $\tau = 0$ and $\tau = 1$ the solutions converge to $\mathcal{E}_1^\dagger$, so the virus survives, but it converges to $\mathcal{E}_0$ in the case of $\tau = 2$, so the infection dies out. In the context of HIV treatment, these dynamical results can be interpreted as a beneficial outcome. For phage-microbe systems, study (Abedon et al. 2001) suggests that increased eclipse stage time is compensated by increasing burst size. To incorporate the compensation, we replace α with $\alpha/e^{-d\tau}$, fixing the value of $\mathcal{R}_0$ despite varying τ. Fig. 6 shows that the change in the persistence (or bistable) region of virus is relatively small. However, the infected cell population size, in particular the C component of both $\mathcal{E}_1^\dagger$, the stable interior equilibrium, and $\mathcal{E}_2^\dagger$, the unstable interior equilibrium, decrease as τ increases.

There are several recent papers that show experimental evidence for the role of cellular proliferation (independent of antigen) in HIV persistence in the latent reservoir. For example, a recently published experimental study (Pinzone et al. 2019) shows that cellular proliferation is an important mechanism for HIV persistence, and suggests that a deeper understanding of these latent reservoirs will be crucial for HIV treatment. In HIV, there is long-lived reservoir of infected cells consisting of various cells such as microphages, T-cells, etc.., which allow for the persistence of HIV under highly active anti-retroviral drug therapy. The question is: *under treatment, how is this HIV reservoir maintained in order to cause persistence of the infection?* A recent study shows cellular proliferation is a major reason allowing persistence. In our model, this can roughly correspond to $\alpha \approx 0$, where there is a very low rate of viral production/budding off. In this work, we explore the condition allowing this reservoir to persist. For example, our numerical results suggest that despite $\mathcal{R}_0 < 1$, the infected cells can persist if the *backward bifurcation condition* (13) holds. Studies have found that a small percentage of people who begin *aggressive combination of antiretroviral* (ARV) treatment shortly after becoming infected have a better chance of controlling the virus for a prolonged period, if they cease the drugs and also have a reduced size of latent reservoirs of infected cells (Ananworanich et al. 2015; Violari et al. 2019). These can be important factors in working toward curing HIV, possibly with the development of latency reversing drugs. Our results can help explain these case studies. For example, Fig. 7 shows that when $\alpha \approx 0$ and infected cell net growth constant rate r_0 is large enough, but less than $r_0 = r_0^c$, depending on the initial infected cell abundance, the virus either eventually get cleared (when infected cell abundance is small) or persists indefinitely, when the abundance is large. Important questions can concern how much of infected cell reservoir should be reduced via latency reversing or the initial seeding (if ARV is started early in infection) to succeed in the eradication of the HIV virus, and whether oscillatory behavior may partially describe observed viral blips.

In the context of phage-microbe systems, we investigate the dual modes of viral reproduction via bifurcation diagrams with respect to r_0 and α in Fig. 7. The two-parameter bifurcation diagram in a) displays several types of bifurcations. In the one parameter diagram with respect to α, the infected cell abundance can decrease with increasing α (and $\mathcal{R}_0$) (see Fig. 7 d)). As viral production increases via increasing viral budding off rate α, the susceptible cell population can be driven to lower levels and eventually to collapse. This might be ultimately detrimental to infected cell prevalence since in the absence of susceptible cells, horizontal transmission (another route of chronic viral infection) does not occur; thus resulting in less infected cell prevalence despite increase in free virus concentration in the environment (see Fig. 7 b)- e)).

Finally in prior studies, (Beretta et al. 2002; Smith 2011; Northcott et al. 2012) it has been shown that the time delay or time in the eclipse stage (Browne 2016) can induce Hopf bifurcations in systems with lytic viral infection, leading to oscillatory dynamics, including stable limit cycles and chaos. Interestingly, for system (1), describing persistent infection among replicating host cells, the numerical results suggest that the delay time and eclipse stage in combination reduces the parameter region, inducing oscillations, in dynamically interacting virus-microbial host populations (see Fig. 3, Fig. 4, and Fig. 8.)

6 Discussion

Here, we introduce a nonlinear time-delay model describing the interactions between persistently infecting viruses and their host cells with time delay in eclipse stage. Analytically we first establish wellposedness of the system and show that the system is dissipative. Later we define biologically interpretable threshold conditions such as $\mathcal{R}_0$ and $\mathcal{R}_S^{C_0}$ and show that the boundary equilibria $\mathcal{E}_0$ (infection-free) and $\mathcal{E}_c$ (chronic-only) are locally asymptotically stable whenever the respective threshold condition is less than one; otherwise they are unstable. In addition, by considering intrinsic infected cell reproduction rate, r_0, as a bifurcation parameter, we derive general conditions for backward (with bistable dynamics) and transcritical bifurcations at critical values r_0^c and r_0^b where the boundary equilibria change stability. Furthermore, we characterize coexistence (interior) equilibrium, along with a simple case of bistability: (i) if $r_0^c < r_0 < r_0^b$, then there is a unique interior equilibrium, (ii) if $r_0 > r_0^b$ and $r_0 > r_0^c$, then the system has no positive interior equilibrium, but stable $\mathcal{E}_c$, (iii) if $r_0^b < r_0 < r_0^c$, then the system presents bistability with both boundary equilibria locally stable. Finally, by using the Lyapunov exponent method, we prove distinct scenarios for robust uniform persistence of virus and infected and susceptible cell populations, referring to long term survival above a positive threshold density, based on $\mathcal{R}_0$ or $\mathcal{R}_S^{C_0}$ being above unity.

Furthermore, by using estimated parameter values in phage-microbe systems, we numerically address how the eclipse stage time delay interacts with dual modes of virus reproduction. We show that the delay time in eclipse stage does not change the types of possible bifurcations, which are shown for corresponding no delay model in the prior study (Gulbudak and Weitz 2019). Yet, we observe that larger delays increase bistable

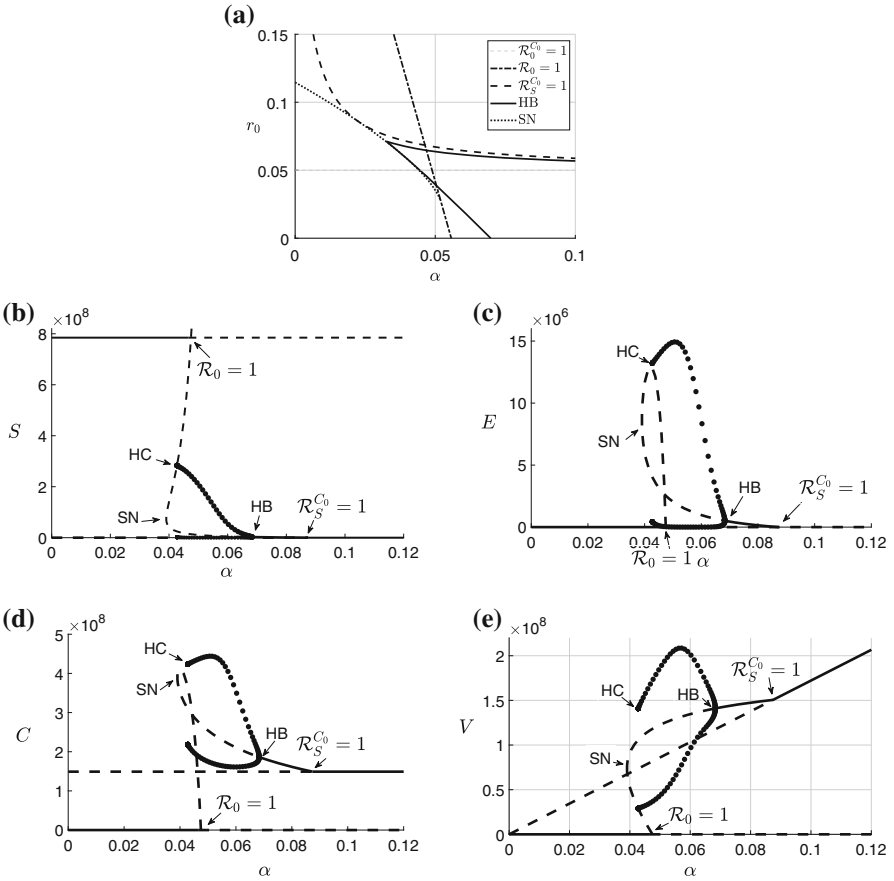

Fig. 7 **a** Two-parameter bifurcation diagram with bifurcation parameters: virus replication rate, α versus chronic cell net growth rate, r_0, the dual modes of virus replication. All parameter values used, apart from the bifurcation parameters, r_0 and α, are given in Table 3, except we set $\tau = 1$ and $\phi = 1.6 \times 10^{-9}$. The saddle-node bifurcation curve is seen to terminate where it intersects the curve where $\mathcal{R}_0 = 1$ at $\alpha \approx 0.0524$. This value was also determined using Maple (Maple 2021) by setting the criterion in Theorem 3 (for determining if the bifurcation is a forward or a backward bifurcation) equal to zero and solving for α. The bifurcation at $r_0 = r_0^c$ ($\mathcal{R}_0 = 1$) is therefore a backward bifurcation for smaller values of α and a forward bifurcation for larger values of α. **b–e** Corresponding one-parameter bifurcation diagrams with $r_0 = 0.06$. The family of periodic solutions born at the Hopf bifurcation (HB) indicated on the graphs terminates at a homoclinic bifurcation (HC). Because the saddle-node (SN) bifurcation is so close to the first Hopf bifurcation, which is very close to another homoclinic bifurcation (HC), these are not visible

region, while persistence can either occur in a narrower or wider range of parameters and initial conditions (dependent upon whether increased eclipse stage time is compensated by increasing burst size). Also interestingly, the Hopf bifurcation region diminishes with delay. These results can have important ecological implications. As the delay time increases, the population dynamics outcomes, including long term survival of viruses and cells, become more sensitive to environmental fluctuations, which can be deleterious or favorable outcome for the host cell and virus population. We inter-

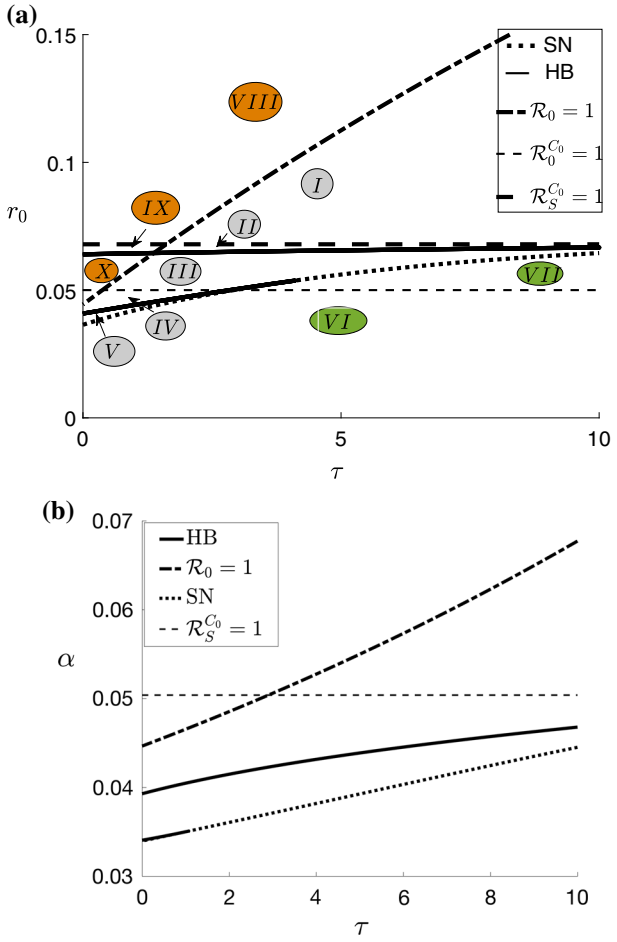

Fig. 8 Two-parameter bifurcation diagrams comparing how time-delay affects the dynamics for the dual modes of replication: with $\alpha = 1/21$ and r_0 as the second bifurcation parameter in a) and $r_0 = 0.6$ and α as the second bifurcation parameter in b). In a), the system displays bistable dynamics in the parameter regions (I-V) labelled in grey, except that there is likely a branch of homoclinic bifurcations emanating from the intersection of the saddle-node bifurcation curve (SN) and the Hopf bifurcation curve (HB). At the intersection there is likely a Bogdanov–Takens bifurcation, and so the periodic solution and hence the bistability is likely to disappear in a subregion of region III. In regions labelled in orange (VIII-X) the infection persists and in regions (VI-VII), labelled in green, it dies out. (b) Again the Hopf bifurcation and the saddle-node bifurcation branches intersect at what is likely a Bogdanov–Takens bifurcation. It is also interesting to observe that even if there is no time delay, there are two values of α for which Hopf bifurcations occur

pret the analytical and numerical results in the context of phage-microbe systems, within-host persistent infections, such as HIV, and tumor oncolytic virotherapy.

In this study, we formulate a modeling framework for viral infections with two modes of replication, namely infected cell proliferation and viral budding, which can apply to temperate phages, persistent viral infections such as HIV latently infected

cells-virus interactions, and oncolytic virotherapy. We used a discrete delay to model the time spent in the eclipse stage, i.e., we considered the Dirac delta distributed delay. However, other distributions might be more realistic. It would be interesting to determine whether the dynamics are sensitive to the form of the delay distribution. We suspect that the range of dynamics observed would remain the same, based on our experience with other models. In particular, in the case of the model of basic competition in the chemostat, in Wolkowicz et al. (1997) the dynamics of the chemostat model with delay in the form of the Gamma distribution was compared with the dynamics of the analogous model with discrete delay studied in Wolkowicz and Xia (1997). At a fairly large order (order 32) of the Gamma distribution, but with the mean delay equal to the discrete delay, the solutions were indistinguishable from the solutions of the model with discrete delay and the range of behavior was identical for all orders of the Gamma distribution. In Teslya and Wolkowicz (2020), a predator-prey model with different forms of distributed delay, i.e., various Gamma distributions and the Uniform distribution were compared with the dynamics observed in the analogous model studied by Fan and Wolkowicz (2021), in the case of discrete delay. All of these models had complex behavior, including chaotic dynamics. However, for all the different distributions, with minor variations, the observed types of bifurcations persisted. Therefore, we expect the range of dynamics to be very similar if discrete delay is replaced by distributed delay in the model studied in this paper. However, in future work, it would be interesting to determine what differences can occur. In other future work, we will consider complexities relevant to particular systems. For example, in the case of HIV, the model (1) can be extended to include productively infected (lytic) state with some probability of switching between the latent (chronic) and active states (Rong and Perelson 2009). Finally, the setting can be generalized to consider evolution of viral populations with distinct infection strategies to inform on the diversity of virus-host cell infection modes observed in nature.

Acknowledgements The authors thank two anonymous reviewers for their helpful comments and feedback on the manuscript, and Cameron Browne of University of Louisiana at Lafayette for his helpful discussions. Hayriye Gulbudak was supported by NSF grant (DMS-1951759) and Simons Foundation/SFARI(638193). The work of Paul Salceanu was supported by a Simons Foundation Collaboration Grant for Mathematicians (Award Number: 524761). The research of Gail S. K. Wolkowicz was partially supported by a Natural Sciences and Engineering Research Council of Canada (NSERC) Discovery grant with accelerator supplement.

A Proofs

A.1 Proof of Theorem 1

Proof To study the behavior of the solutions near an equilibrium, we first linearize the model (1) about the equilibrium $(S^*,\ E^*,\ C^*,\ P^*)$ by taking $S(t) = S^* + x(t)$, $E(t) = E^* + y(t)$, $C(t) = C^* + z(t)$, and $V(t) = V^* + v(t)$. We look for eigenvalues of the linear operator - that is we look for solutions of the form $x(t) = \overline{x}e^{\lambda t}$, $y(t) = \overline{y}e^{\lambda t}$, $z(t) = \overline{z}e^{\lambda t}$, and $v(t) = \overline{v}e^{\lambda t}$, where $\lambda \in \mathbb{C}$ and $\overline{x},\ \overline{y},\ \overline{z},\ \overline{v}$ are arbitrary non-zero constants, but the eigenvalue λ is common. This process results in the following

system (the bars have been omitted):

$$\begin{cases} \lambda x &= -rS^*\dfrac{n}{K} + rx\left(1-\dfrac{N^*}{K}\right) - \phi S^* v - \phi x V^* - dx \\ \lambda y &= \phi S^* v + \phi x V^* - \hat{d}y - \phi e^{-\hat{d}\tau} S^* v e^{-\lambda\tau} - \phi e^{-\hat{d}\tau} x e^{-\lambda\tau} V^*, \\ \lambda z &= -r_0 C^*\dfrac{n}{K} + r_0 z\left(1-\dfrac{N^*}{K}\right) - \tilde{d}z + \phi e^{-\hat{d}\tau} S^* v e^{-\lambda\tau} + \phi e^{-\hat{d}\tau} x e^{-\lambda\tau} V^*, \\ \lambda v &= \alpha z - \phi S^* v - \phi x V^* - \mu v, \end{cases} \tag{15}$$

where $N^* = S^* + E^* + C^*$ and $n = x + y + z$.
At the equilibrium, $\mathcal{E}_0 = (S_0, 0, 0, 0)$, system (15) simplifies to:

$$\begin{cases} \lambda x &= -rS_0\dfrac{n}{K} + rx\left(1-\dfrac{S_0}{K}\right) - \phi S_0 v - dx \\ \lambda y &= \phi S_0 v - \hat{d}y - \phi e^{-\hat{d}\tau} S_0 v e^{-\lambda\tau}, \\ \lambda z &= r_0 z\left(1-\dfrac{S_0}{K}\right) - \tilde{d}z + \phi e^{-\hat{d}\tau} S_0 v e^{-\lambda\tau}, \\ \lambda v &= \alpha z - \phi S_0 v - \mu v. \end{cases} \tag{16}$$

We obtain the following characteristic equation:

$$1 = \frac{r_0}{(\tilde{d}+\lambda)}\left(1-\frac{S_0}{K}\right) + \frac{\phi S_0 e^{-(\hat{d}+\lambda)\tau}}{\lambda+\phi S_0+\mu}\frac{\alpha}{(\tilde{d}+\lambda)}. \tag{17}$$

Let

$$G(\lambda) = \frac{r_0}{(\tilde{d}+\lambda)}\left(1-\frac{S_0}{K}\right) + \frac{\phi S_0 e^{-(\hat{d}+\lambda)\tau}}{\lambda+\phi S_0+\mu}\frac{\alpha}{(\tilde{d}+\lambda)}.$$

First, we show that if $\mathcal{R}_0 > 1$, then (17) has a positive real solution, and hence $\mathcal{E}_0$ is unstable. Since $S_0 < K$, it follows that $G(\lambda)$ is a decreasing function of $\lambda \in \mathbb{R}$. Note also that $\lim_{t\to\infty} G(\lambda) = 0$. Therefore, if $G(0) > 1$, there exists $\lambda^* > 0$ such that $G(\lambda^*) = 1$. Since $G(0) = \mathcal{R}(0) > 1$, it follows that (17) has a positive solution, and hence $\mathcal{E}_0$ is unstable.

Next, assume that $\mathcal{R}_0 < 1$. Since, $S_0 < K$, we have $0 < G(0) = \mathcal{R}_0 < 1$. By continuity, there exists $0 < \sigma < \min\{\tilde{d}, \hat{d}, \mu\}$, such that $|G(-\sigma)| < 1$. If $\lambda = a + ib$ and $a \geq -\sigma$, then since $\tilde{d} - \sigma > 0$ and $\mu - \sigma > 0$,

$$\begin{aligned} |G(\lambda)| &\leq \left|\frac{1}{\tilde{d}+a+ib}\right|\left[\left|r_0\left(1-\frac{S_0}{K}\right)\right| + \left|\alpha\frac{\phi S_0 e^{-(\hat{d}+a+ib)\tau}}{\phi S_0+(\mu+a+ib)}\right|\right] \\ &\leq \left|\frac{1}{\tilde{d}+a+ib)}\right|\left(r_0\left(1-\frac{S_0}{K}\right) + \alpha\frac{\left|\phi S_0 e^{-(\hat{d}+a+ib)\tau}\right|}{|\phi S_0+(\mu+a+ib)|}\right) \end{aligned}$$

$$
\begin{aligned}
&\leq \left|\frac{1}{\tilde{d}-\sigma)}\right|\left(r_0\left(1-\frac{S_0}{K}\right)+\alpha\frac{\left|\phi S_0 e^{-(\hat{d}+a)\tau}\right|}{|\phi S_0+(\mu+a+ib)|}\right)\\
&\leq \left|\frac{1}{\tilde{d}-\sigma)}\right|\left(r_0\left(1-\frac{S_0}{K}\right)+\alpha\frac{\phi S_0 e^{-(\hat{d}+a)\tau}}{\phi S_0+(\mu+a)}\right)\\
&\leq \left|\frac{1}{\tilde{d}-\sigma)}\right|\left(r_0\left(1-\frac{S_0}{K}\right)+\alpha\frac{\phi S_0 e^{-(\hat{d}-\sigma)\tau}}{\phi S_0+(\mu-\sigma)}\right)\\
&= |G(-\sigma)|<1.
\end{aligned}
$$

Hence one can conclude that $\sup\{Re\lambda : G(\lambda)=1\} < -\sigma$. The conclusion follows from Theorem 4.8 in Smith (Smith 2011). □

A.2 Proof of Theorem 2

Proof We consider the local stability of $\mathcal{E}_c$. Evaluated at this equilibrium, (15) becomes,

$$
\begin{cases}
\lambda x &= rx(1-\dfrac{C_0}{K})-\phi x V_c - dx,\\
\lambda y &= \phi x V_c - \hat{d}y - \phi e^{-\hat{d}\tau}xe^{-\lambda\tau}V_c,\\
\lambda z &= -r_0 C_0\dfrac{n}{K}+r_0 z(1-\dfrac{C_0}{K})-\tilde{d}z+\phi e^{-\hat{d}\tau}xe^{-\lambda\tau}V_c,\\
\lambda v &= \alpha z-\phi x V_c-\mu v.
\end{cases}
\tag{18}
$$

Since $V_c=\dfrac{\alpha}{\mu}C_0$, the characteristic equation is given by

$$
[-\mu-\lambda]\left[-\hat{d}-\lambda\right]\left[r_0\left(1-\frac{C_0}{K}\right)-\tilde{d}\right]\left[r\left(1-\frac{C_0}{K}\right)-\phi\frac{\alpha}{\mu}C_0-d-\lambda\right]=0,
$$

a polynomial of degree 4 with roots:

$$
\lambda_1=-\mu,\quad \lambda_2=-\hat{d},\quad \lambda_3=-r_0+\tilde{d},\quad \lambda_4=r\left(1-\frac{C_0}{K}\right)-\phi\frac{\alpha}{\mu}C_0-d
$$

λ_1 and λ_2 are always negative. λ_3 is negative provided $C_0 > 0$, i.e., when $\mathcal{E}_c$ is biologically relevant.

$$
\begin{aligned}
\lambda_4 &= C_0\left[r\left(\frac{1}{C_0}-\frac{1}{K}\right)-\phi\frac{\alpha}{\mu}-\frac{d}{C_0}\right]=C_0\left[\frac{r-d}{C_0}-\frac{r}{K}-\frac{K\phi\alpha}{r\mu}\right]\\
&=\frac{rC_0}{K}\left[\frac{S_0}{C_0}-\frac{K\phi\alpha}{r\mu}-1\right]=\frac{rC_0}{K}\left[\mathcal{R}_S^{C_0}-1\right].
\end{aligned}
$$

Therefore, when $\mathcal{E}_c$ is biologically meaningful, it is locally asymptotically stable if $\mathcal{R}_S^{C_0} < 1$ and unstable if $\mathcal{R}_S^{C_0} > 1$. □

A.3 Proof of Proposition 1.

Proof Let

$$\mathcal{E}_i^\dagger = (S_i^\dagger, E_i^\dagger, C_i^\dagger, V_i^\dagger) : \mathcal{E}_i^\dagger \in \mathbb{R}^4_{>0},\ i = 1, 2$$

denote the interior equilibria of system (1), provided they exist. Then, if we define

$$N_i^\dagger = S_i^\dagger + E_i^\dagger + C_i^\dagger, \tag{19}$$

equating the right-hand sides of (1) equal to zero to obtain expressions for the components of the equilibria, it follows that

$$N_i^\dagger = S_0 - \frac{K}{r}\phi V_i^\dagger,\ V_i^\dagger = \frac{\alpha C_i^\dagger}{\phi S_i^\dagger + \mu},\ E_i^\dagger = \frac{\phi S_i^\dagger}{\phi S_i^\dagger + \mu}\frac{\alpha C_i^\dagger}{\hat{d}}[1 - e^{-\hat{d}\tau}]. \tag{20}$$

and

$$0 = \frac{r_0 C_0}{K} C_i^\dagger (1 - \frac{N_i^\dagger}{C_0}) + \phi e^{-\hat{d}\tau} S_i^\dagger V_i^\dagger. \tag{21}$$

Substituting both equations for $N_i^\dagger$ and $V_i^\dagger$ in (20) into equation (21), we obtain (7), i.e.,

$$C_i^\dagger = S_i^\dagger (B - \frac{r e^{-\hat{d}\tau}}{r_0}) + \frac{\mu}{\phi} B, \quad \text{where} \quad B = \frac{r}{K\alpha}[S_0 - C_0]. \tag{22}$$

In addition, substituting the expression for $E_i^\dagger$ in (20) and the expression for $C_i^\dagger$ in (7) into (19),

we obtain,

$$N_i^\dagger = S_i^\dagger + \left[S_i^\dagger (B - \frac{r e^{-\hat{d}\tau}}{r_0}) + \frac{\mu}{\phi} B \right] \left[1 + \frac{\phi S_i^\dagger}{\phi S_i^\dagger + \mu} \frac{\alpha}{\hat{d}} [1 - e^{-\hat{d}\tau}] \right]. \tag{23}$$

Then, by substituting the expression for $V_i^\dagger$ in (20) into (21), we obtain

$$N_i^\dagger = \frac{\alpha \phi S_i^\dagger e^{-\hat{d}\tau} K}{(\phi S_i^\dagger + \mu) r_0} + C_0. \tag{24}$$

By equating (23) and (24), we obtain

$$S_i^\dagger + \left[S_i^\dagger (B - \frac{re^{-\hat{d}\tau}}{r_0}) + \frac{\mu}{\phi} B \right] \left[1 + \frac{\phi S_i^\dagger}{\phi S_i^\dagger + \mu} \frac{\alpha}{\hat{d}} [1 - e^{-\hat{d}\tau}] \right] = \frac{\alpha \phi S_i^\dagger e^{-\hat{d}\tau} K}{(\phi S_i^\dagger + \mu) r_0} + C_0. \tag{25}$$

Rearranging equation (25), we obtain $h(S^\dagger)_i = g(S_i^\dagger)$, where

$$\begin{aligned} h(S_i^\dagger) &= S_i^\dagger [\phi S_i^\dagger + \mu] + \left[S_i^\dagger (B - \frac{re^{-\hat{d}\tau}}{r_0}) + \frac{\mu}{\phi} B \right] \\ &\quad \left[(\phi S_i^\dagger + \mu) + \phi S_i^\dagger \frac{\alpha}{\hat{d}} [1 - e^{-\hat{d}\tau}] \right], \quad \text{and} \\ g(S_i^\dagger) &= \frac{\alpha \phi S_i^\dagger e^{-\hat{d}\tau} K}{r_0} + C_0 (\phi S_i^\dagger + \mu). \end{aligned} \tag{26}$$

Note that $g(S_i^\dagger)$ is a linear increasing function and $h(S_i^\dagger)$ is a quadratic polynomial. Therefore, these two curves can have at most two intersection points, and hence there are at most two possible candidates for $S_i^\dagger$ and only real, positive roots are candidates for the component of an interior equilibrium.

First rearranging equation (26), and then simplifying the expressions of coefficients (verified also by the symbolic package Maple [32]), we obtain the quadratic polynomial (5), with coefficients defined in (6). Using (20), to find the corresponding $E_i^\dagger$ and $V_i^\dagger$, it follows that $\mathcal{E}_i^\dagger$ is an interior equilibrium of system (1) whenever $S_i^\dagger > 0$ and the corresponding expression given in (7) for $C_i^\dagger > 0$. Hence, there can be at most two interior equilibria.

Alternatively, we can find the quadratic equation (9) for the $C_i^\dagger$ component of $\mathcal{E}_i^\dagger$ by first rearranging (7) to find the expression for $S_i^\dagger$ as a function of $C_i^\dagger$ and substituting this expression into (26). Then by simplifying the coefficients by multiplying the equation (verified also by Maple [32]) by $\phi \alpha r_0^2 \left(B - \frac{re^{-\hat{d}\tau}}{r_0} \right)^2$ and rearranging them, we obtain the expressions for the coefficients in (10). □

A.4 Proof of Theorem 3

Proof To determine whether there is a forward or a backward bifurcation when $r_0 = r_0^c$, we find the sign of the derivative of the component $C^\dagger$ of $\mathcal{E}^\dagger$ with respect to r_0 at $r_0 = r_0^c$, the transcritical bifurcation involving $\mathcal{E}_0$ and $\mathcal{E}^\dagger$, where these two equilibria cross and exchange stability, i.e., where $\mathcal{E}^\dagger = \mathcal{E}_0$, and so $C^\dagger = 0$.

By Lemma 1, we know that $B - \frac{re^{-\hat{d}\tau}}{r_0} \neq 0$ near $r_0 = r_0^c$. Therefore by Proposition 1, the C component of $\mathcal{E}^\dagger$, must satisfy $P(C^\dagger) = 0$ near r_0^c, where $P(C)$ is defined in (9) with coefficients defined in (10).

First by the Implicit Function Theorem, we will guarantee that whenever $a_1(r_0^c) \neq 0$, there exists an open interval set $\mathcal{U}$ of $\mathbb{R}$, containing r_0^c, such that there exists a unique continuously differentiable function, $f : \mathcal{U} \to \mathbb{R}$, where

$$f(r_0^c) = 0, \text{ and } P(r_0, f(r_0))) = 0, \ \forall r_0 \in \mathcal{U}.$$

Differentiating $P(C) = 0$ implicitly with respect to r_0 (noting that the coefficients depend on r_0), and evaluating at r_0^c, where $C^\dagger = 0$, we obtain

$$\frac{dC^\dagger}{dr_0}|_{(r_0=r_0^c, C^\dagger=0)} = \frac{-\frac{\partial a_2}{\partial r_0}(r_0^c)}{a_1(r_0^c)}. \tag{27}$$

Therefore if $a_1(r_0^c) \neq 0$, we can conclude that $C^\dagger(r_0)$, given in (7), is a unique (and continuously differentiable) function of r_0 on an open neighborhood of the point r_0^c. Next we will check the sign of the derivative, given in (27), and complete the proof.

Now since,

$$\frac{\partial a_2}{\partial r_0}(r_0^c) = -\mu d e^{-\hat{d}\tau}(K\phi(r-d) + \mu r) < 0, \tag{28}$$

the sign of the derivative in (27) is the same as the sign of $a_1(r_0^c)$. Using Maple to evaluate $a_1(r_0^c)$ and defining the positive factor

$$\omega(r_0^c) = \frac{\mu\phi\alpha e^{-\hat{d}\tau}}{d\hat{d}(S_0\phi + \mu)^2}$$

it follows that

$$\begin{aligned}\frac{a_1(r_0^c)}{\omega(r_0^c)} = e^{-\hat{d}\tau}\left(\alpha\hat{d}r^2\phi^2 S_0^2 + d\hat{d}\mu^2 r^2 + rK\mu\phi\left\{r[\hat{d}(d+\alpha) + \alpha d] - d^2(\alpha+\hat{d})\right\}\right) \\ -r^2 d\mu\phi\alpha S_0 e^{-2\hat{d}\tau} - r^2\hat{d}\tilde{d}(\phi S_0 + \mu)^2,\end{aligned} \tag{29}$$

the expression in (13). Thus, if $a_1(r_0^c) < 0$, the transcritical bifurcation at r_0^c is a backward bifurcation and if $a_1(r_0^c) > 0$, it is a forward bifurcation. □

A.5 Proof of Theorem 4

Proof First we show that when $r = r_0^b$, the equilibria $\mathcal{E}_c$ and $\mathcal{E}^\dagger$ coalesce, i.e., $S^\dagger = 0$, $E^\dagger = 0$, $C^\dagger = C_0$ and $V^\dagger = V_c$. Recall that $S^\dagger$ satisfies equation (5) with coefficients defined in (6):

$$\hat{P}(S^\dagger) = A_0(S^\dagger)^2 + A_1 S^\dagger + A_2 = 0.$$

If $S^\dagger = 0$, $\hat{P}(0) = 0$ if and only if $A_2 = 0$. That is precisely when $\mathcal{R}_S^{C_0} = 1$ or equivalently, when $r_0 = r_0^b$. Note that by similar arguments in the Proof of Theorem 3,

which is given in (A.4), the Implicit Function Theorem guarantees that the function $S^\dagger(r_0)$, given in (7), is unique (and continuously differentiable) function of r_0 on an open neighborhood of the point r_0^b, when $A_1(r_0^b) \neq 0$. Setting $\hat{P}(S^\dagger) = 0$ and differentiating both sides implicitly with respect to r_0, noting that $S^\dagger = 0$ when $r_0 = r_0^b$, it follows that

$$\frac{dS^\dagger}{dr_0}(r_0^b, 0) = -\frac{\frac{\partial A_2}{\partial r_0}(r_0^b)}{A_1(r_0^b)} = \frac{\mu\tilde{d}(K\phi\alpha + \mu r)}{\alpha\phi(r_0^b)^2}\left(\frac{1}{A_1(r_0^b)}\right),$$

and hence the sign of this expression depends on the sign of A_1, evaluated at $r_0 = r_0^b$. Using MAPLE to evaluate $A_1(r_0^b)$,

it follows that

$$A_1(r_0^b) = \frac{(-d\hat{d}\mu^2 r - K\phi\alpha\mu(\hat{d}(d+r) + \tilde{d}(r-d)) - (K\phi\alpha)^2\hat{d})e^{-\hat{d}\tau} - \mu\tilde{d}(-\hat{d}\mu r + K\phi((d-r-\hat{d})\alpha + \hat{d}(d-r)))}{\tilde{d}\hat{d}(K\phi\alpha + \mu r)} \tag{30}$$

Thus, if $A_1(r_0^b) > 0$, the transcritical bifurcation at r_0^b is a backward bifurcation and if $A_1(r_0^b) < 0$, it is a forward bifurcation. □

A.6 Proof of Theorem 5

Lemma 2 *Consider $B(r_0)$, given in (7), and define $r_0^* = \frac{r\tilde{d}}{d}$. Then, $B(r_0^*) = 0$. If $r_0 < r_0^*$, then $B(r_0) > 0$ and if $r_0 > r_0^*$, then $B(r_0) < 0$. Furthermore,* $\max\{r_0^c, r_0^b\} < r_0^*$.

Proof Note that $B = \frac{r}{K\alpha}[S_0 - C_0] = \frac{r\tilde{d} - r_0 d}{\alpha r_0} = \frac{d(r^* - r_0)}{\alpha r_0}$. Therefore, $B(r_0^*) = 0$. In addition,

$B(r_0) > 0$ for all $r_0 < r_0^*$ and $B(r_0) < 0$ for all $r_0 > r_0^*$. Also note that $r_0^* - r_0^c = \frac{r\phi\alpha S_0 e^{-\hat{d}\tau}}{d(\phi S_0 + \mu)} > 0$ and $r_0^* - r_0^b = \frac{r\phi\alpha\tilde{d}S_0}{d(K\phi\alpha + d\mu)} > 0$. Therefore, $r_0^* > \max\{r_0^c, r_0^b\}$. □

Lemma 3 **(a)** *The function $\mathcal{R}_0(r_0)$, defined in (3), is continuous and increasing for $r_0 > 0$.*

i) If $r_0 < r_0^c$, then $a_2(r_0) > 0$.
ii) If $r_0 > r_0^c$, then $a_2(r_0) < 0$.

(b) $r_0^b > \tilde{d}$.

(c) *$A_2(r_0)$, defined in (6), has a removeable singularity at $r_0 = \tilde{d}$ and can be redefined by multiplying C_0 into the term in square brackets so that it is differentiable and decreasing for all $r_0 > 0$.*

i) If $0 < r_0 < r_0^b$, then $A_2(r_0) > 0$.
ii) If $r_0 > r_0^b$, then $A_2(r_0) < 0$.

Proof **(a)** This follows directly from the definition of $\mathcal{R}_0$ in (3), the definition of r_0^c in (11), and the definition of a_2 in (10).

(b) Note that

$$r_0^b - \tilde{d} = \frac{\tilde{d}\mu r S_0}{K^2\phi\alpha + d\mu} > 0.$$

(c) The function $\mathcal{R}_S^{C_0}(r_0)$, defined in (4), has a vertical asymptote at $r_0 = \tilde{d}$. $\mathcal{R}_S^{C_0}(r_0) < 0$ if $r_0 < \tilde{d}$, Multiplying C_0 into the expression in square brackets in (6) and simplifying we obtain,

$$A_2(r_0) = \frac{\mu^2 r C_0}{\phi K\alpha}[R_S^{C_0} - 1] = \frac{\mu(K\phi\alpha(\tilde{d} - r_0) - (r_0 d - r\tilde{d}))}{r_0\phi\alpha}, \tag{31}$$

and

$$\frac{dA_2(r_0)}{dr_0} = \frac{-\tilde{d}\mu(K\phi\alpha + \mu r)}{r_0^2\phi\alpha} < 0.$$

Substituting $r_0 = \tilde{d}$ into (31), since $r > d$, it follows that $A_2(r_0)|_{r_0=\tilde{d}} > 0$. If $0 < r_0 < \tilde{d}$ then both $C_0(r_0)$ and $\mathcal{R}_S^{C_0}(r_0)$ are negative and it follows again that $A_2(r_0) > 0$. However, if $r_0 > \tilde{d}$, then $C_0(r_0) > 0$, and the sign of $A_2(r_0)$ depends upon whether or not $\mathcal{R}_S^{C_0}(r_0)$ is larger or smaller than 1, and hence whether $r_0 > r_0^b$ or $r_0 < r_0^b$. Therefore, if $r_0 > r_0^b$, then $A_2(r_0) < 0$ and if $\tilde{d} < r_0 < r_0^b$, then $A_2(r_0) > 0$.

□

We denote the coefficient of S in (7) by

$$B_c(r_0) := B(r_0) - \frac{re^{-\hat{d}\tau}}{r_0}. \tag{32}$$

Lemma 4 *If $A_0(r_0) \leq 0$, where $A_0(r_0)$ is defined in (6), then $B_c(r_0) < 0$.*

Proof $A_0 = \frac{\phi}{\hat{d}}\left(\alpha B_c(1 - e^{-\hat{d}\tau}) + \hat{d}(B_c + 1)\right)$. □

Lemma 5 *Assume $A(\widehat{r_0}) = 0$. If either $\alpha \neq \tilde{d}e^{\hat{d}\tau}$ or $\tilde{d} \neq \frac{d\hat{d}e^{-\hat{d}\tau}}{\hat{d} - d(1-e^{-\hat{d}\tau})}$, then $\frac{dA_0(\widehat{r_0})}{dr_0} \neq 0$. Otherwise, $A(r_0) = 0$ (and $a_0(r_0) = 0$) for all $r_0 \geq 0$.*

Proof If $A_0(\widehat{r_0}) = 0$, then

$$r(\tilde{d} - \alpha e^{-\hat{d}\tau})\left(1 - \frac{\alpha(e^{-\hat{d}\tau} - 1)}{\hat{d}}\right) = \widehat{r_0}\left(d(1 - \frac{\alpha(e^{-\hat{d}\tau} - 1)}{\hat{d}}) - \alpha\right). \tag{33}$$

If the coefficient of $\widehat{r}_0$ in (33) equals zero, one of the factors on the left hand side of (33) must equal zero. It cannot be the one in the large brackets, since then coefficient of $\widehat{r}_0$ would equal $-\alpha$ with equality if and only if $\alpha = 0$, yielding a contradiction. Therefore, the other factor on the left hand side must equal 0, i.e., $\alpha = \tilde{d}e^{\hat{d}\tau}$. Then, substituting this value of α into the coefficient of $\widehat{r}_0$ in (33) setting the coefficient equal to zero, it follows that

$$\tilde{d} = \frac{d\hat{d}e^{-\hat{d}\tau}}{\hat{d} - d(1 - e^{-\hat{d}\tau})} \tag{34}$$

Therefore, as long as $\alpha \neq \tilde{d}e^{\hat{d}\tau}$ or condition (34) does not hold, then the coefficient of $\widehat{r}_0$ in (33) is nonzero and so $\frac{dA_0(r_0)}{dr_0}|_{r_0=\widehat{r}} \neq 0$. Otherwise, $A_0(r_0) = 0$ for all r_0. □

Definition 1 When

$$\alpha = \tilde{d}e^{\hat{d}\tau} \quad \text{and} \quad \tilde{d} = \frac{d\hat{d}e^{-\hat{d}\tau}}{\hat{d} - d(1 - e^{-\hat{d}\tau})} \tag{35}$$

we refer to this as *the degenerate case*.

Lemma 6 *Assume (35) is satisfied. Then,* $r_0^c > 0$, *and*

i) $\hat{d}K\phi - \mu r(1 - e^{-\hat{d}\tau}) > 0$, *if and only if* $r_0^c < r_0^b$.
ii) $\hat{d}K\phi - \mu r(1 - e^{-\hat{d}\tau}) = 0$, *if and only if* $r_0^c = r_0^b$.
iii) $\hat{d}K\phi - \mu r(1 - e^{-\hat{d}\tau}) < 0$, *if and only if* $r_0^c > r_0^b$.

Proof We substitute the values for α and $\tilde{d}$ given in (35) into the expressions for r_0^c and r_0^b given in (11) and (12), respectively.

$$r_0^c = \frac{d\hat{d}\mu r^2 e^{-\hat{d}\tau}}{(\hat{d} - d(1 - e^{-\hat{d}\tau}))(\mu r + K\phi(r - d))} > 0,$$

since $r > d$ and $\tilde{d} > 0$, and so the denominator in the expression for $\tilde{d}$ in (35) is therefore positive. Also, by Lemma 3(b), $r_0^b > \tilde{d} > 0$.

Next we evaluate $r_0^b - r_0^c$ to obtain:

$$r_0^b - r_0^c = \left[\hat{d}K\phi - \mu r(1 - e^{-\hat{d}\tau})\right]\left(\frac{d\hat{d}\,\phi e^{-\hat{d}\tau} S_0}{(\hat{d}K\phi + \mu(\hat{d} - d(1 - e^{-\hat{d}\tau}))(\hat{d} - d(1 - e^{-\hat{d}\tau}))(\phi S_0 + \mu)}\right). \tag{36}$$

All of the factors in the expression in the large round brackets in (36) are positive, and hence, the sign of (35) is determined by the factor in the square brackets, and the result follows. □

Lemma 7 *Assume that (35) holds.*

i) $a_1(r_0) = -d\phi r_0 A_1(r_0)$ *for all* r_0.

ii) $A_1(r_0)$, $a_1(r_0)$, *and* $a_2(r_0)$ *are all continuous functions of* $r_0 > 0$ *and* $A_2(r_0)$ *has a removeable singularity at* $r_0 = \tilde{d}$ *and can be defined so that it is continuous for all* $r_0 > 0$.

iii) $A_1(r_0)$, $A_2(r_0)$, *and* $a_2(r_0)$ *are decreasing functions of* $r_0 > 0$ *and* $a_1(r_0)$ *is increasing for* $r_0 > 0$.

iv) $A_1(r_0) < 0$ *if* $r_0^c < r_0 < r_0^b$ *and* $A_1(r_0) > 0$ *if* $r_0^b < r_0 < r_0^c$.

v) $a_1(r_0) > 0$ *if* $r_0^c < r_0 < r_0^b$ *and* $a_1(r_0) < 0$ *if* $r_0^b < r_0 < r_0^c$.

vi) $\hat{P}(S) = A_1(r_0)S + A_2(r_0) = 0$ *has a unique positive solution if* $r_0^c < r_0 < r_0^b$ *and if* $r_0^b < r_0 < r_0^c$.

vii) $P(C) = a_1(r_0)C + a_2(r_0) = 0$ *has a unique positive solution if* $r_0^c < r_0 < r_0^b$ *and if* $r_0^b < r_0 < r_0^c$.

viii) If $r_0 \notin (\min\{r_0^c, r_0^b\}, \max\{r_0^c, r_0^b\})$, *then the solution of at least one of the equations* $\hat{P}(S) = A_1(r_0)S + A_2(r_0) = 0$ *or* $P(C) = a_1(r_0)C + a_2(r_0) = 0$ *is not positive.*

Proof *i)*

$$\frac{-a_1(r_0)}{d\phi r_0^2} = A_1(r_0)$$
$$= \frac{e^{-\hat{d}\tau}[r_0 d(2d\mu - \hat{d}(K\phi + 2\mu)) + \hat{d}^2\mu r] - r_0[d^2\mu e^{-2\hat{d}\tau} + (\hat{d} - d)(\hat{d}K\phi + \mu(\hat{d} - d))]}{r_0\hat{d}(\hat{d} - d(1 - e^{-\hat{d}\tau}))} \quad (37)$$

ii) Noting that we only consider when $\tilde{d} > 0$, and in the degenerate case $\tilde{d}$ satisfies (35), the factor in the denominator of $\tilde{d}$ given in (37) must be positive. It follows that $a_1(r_0)$ and $A_1(r_0)$ are both continuous with respect to r_0, for all $r_0 > 0$.
The singularity in $A_2(r_0)$at $r_0 = \tilde{d}$, where both $C_0 = 0$ and $\mathcal{R}_S^{C_0}(r_0) = 0$ is removed by multiplying C_0 into the term in the square brackets and is continuous with respect to $r_0 > 0$ and $a_2(r_0)$ is clearly continuous with respect to r_0.

iii)

$$\frac{dA_1(r_0)}{dr_0} = \frac{-r\mu\hat{d}e^{-\hat{d}\tau}}{r_0^2(\hat{d} - d(1 - e^{\hat{d}\tau}))} < 0. \quad (38)$$

Therefore, $A_1(r_0)$ is a decreasing function of r_0 and hence by *i)*, $a_1(r_0)$ is an increasing function of r_0.

$$\frac{dA_2(r_0)}{dr_0} = \frac{-\mu e^{-\hat{d}\tau}(d\hat{d}K\phi + \mu r(\hat{d} - d(1 - e^{\hat{d}\tau}))}{r_0^2\phi(\hat{d} - d(1 - e^{-\hat{d}\tau}))} < 0. \quad (39)$$

Therefore, $A_2(r_0)$ is a decreasing function of r_0.

$$\frac{da_2(r_0)}{dr_0} = -e^{-\hat{d}\tau}\mu d(K\phi(r - d) + \mu r) < 0,$$

and hence $a_2(r_0)$ is decreasing function of r_0.

iv) $A_1(r_0^c)$ and $A_1(r_0^b)$ have the same sign or are both equal to zero, since

$$A_1(r_0^b) = \frac{-d(\hat{d}K\phi - \mu r(1-e^{-\hat{d}\tau}))(\hat{d}K\phi + \mu(\hat{d} - d(1-e^{-\hat{d}\tau})))}{d\hat{d}K\phi + \mu r(\hat{d} - d(1-e^{-\hat{d}\tau}))}, \quad (40)$$

$$A_1(r_0^c) = \frac{-d(\hat{d}K\phi - \mu r(1-e^{-\hat{d}\tau}))}{r\hat{d}}. \quad (41)$$

By Lemma 6, $r_0^c > 0$ and so $A_1(r_0)$ is continuous for all $r_0 \geq r_0^c$. By Lemma 6 *i)*, if $r_0^c < r_0 < r_0^b$, then $A_1(r_0^c) < 0$, and by part *iii)* $A_1(r_0)$ is a decreasing function of r_0. Therefore, $A_1(r_0) < 0$ for all $r_0 \in [r_0^c, r_0^b]$.
By Lemma 6 *iii)*, if $r_0^b < r_0 < r_0^c$, then $A_1(r_0^c) > 0$ and by part *iii)* $A_1(r_0)$ is a decreasing function of r_0, and therefore $A_1(r_0) > 0$ for all $r_0 \in [r_0^b, r_0^c]$.

v) By *i)*, $a_1(r_0)$ and $A_1(r_0)$ have opposite signs or are both equal to zero. By *iv)* $A_1(r_0) < 0$ if $r_0^c < r_0^b$. Therefore, $a_1(r_0) > 0$ for all $r_0 \in (r_0^c, r_0^b)$.
Similarly, $a_1(r_0) < 0$ for all $r_0^b < r_0 < r_0^c$.

vi) Since $\hat{P}(S) = 0$ is linear, and by *iv)* and Lemma 3 (c), the coefficients have opposite signs, there is a unique positive solution.

vii) Since $P(C) = 0$ is linear, and by *v)* and Lemma 3 (a), the coefficients have opposite signs, there is a unique positive solution.

viii) First, consider when $0 < r_0 < r_0^b < r_0^c$. By Lemma 3 (a)*i)*, $a_2(r_0) > 0$ and by (c)*i)* $A_2(r_0) > 0$. Next consider when $0 < r_0 < r_0^c < r_0^b$. By Lemma 3 (a)*ii)*, $a_2(r_0) < 0$ and by (c)*ii)* $A_2(r_0) < 0$. In both cases, $a_2(r_0)$ and $A_2(r_0)$ have the same sign. Howeve, from *i)*, $a_1(r_0)$ and $A_1(r_0)$ have opposite signs or are both equal to zero. Therefore, either $A_1(r_0)$ and $A_2(r_0)$ have the same sign and so the solution of $\hat{P}(S) = 0$ is negative, or $a_1(r_0)$ and $a_2(r_0)$ have the same sign and the solution of $P(C) = 0$ is negative or $A_1(r_0) = a_1(r_0) = 0$ and $\hat{P}(S) = 0$ and $P(C) = 0$ has no solution.
In the case that $r_0 > \max\{r_0^c, r_0^b\}$, The result also follows by a similar argument.

□

Proof of Theorem 5 Note that by their definitions in (6) and (10), $A_0(r_0)$ and $a_0(r_0)$ have the same sign or are both equal to zero.

Case (a). Since $r_0 \in (r_0^c, r_0^b)$, by Lemma 3(a), $a_2(r_0) < 0$ and by (c) $A_2(r_0) > 0$.

First assume that $A_0(r_0) > 0$ **and hence** $a_0(r_0) > 0$. Since $A_0(r_0) > 0$ and $A_2(r_0) > 0$, the quadratic equation $\hat{P}(S) = 0$, defined in (5), is concave up and has a positive vertical intercept, and therefore either has two real solutions of the same sign or two complex solutions. On the other hand, since $a_2(r_0) < 0$, the quadratic equation $P(C) = 0$, defined in (9), is concave up and has a negative vertical intercept, and therefore has one negative solution and one positive solution. Therefore there is a most one interior equilibrium. Rearranging (7), we obtain

$$S = \frac{C - \frac{\mu}{\phi}B(r_0)}{B(r_0) - \frac{re^{-\hat{d}\tau}}{r_0}} = \frac{C - \frac{\mu}{\phi}B(r_0)}{B_c(r_0)}, \quad (42)$$

where the denominator is negative, since by Lemma 1, $\bar{r}_0 < r_0^c$. Also, by Lemma 2, $B(r_0) > 0$, since $r_0^* > r_0^b$. Substituting the negative solution of $P(C) = 0$ into (42) gives a corresponding positive value for S. Therefore, the negative solution of $P(C) = 0$ corresponds to a positive solution of $\hat{P}(S) = 0$, and since both solutions of $\hat{P}(S) = 0$ have the same sign, both solutions of $\hat{P}(S) = 0$ must be positive, and so the positive solution of $P(C) = 0$ must also give a positive solution of (42). By (8), the corresponding values of $E^\dagger$ and $V^\dagger$ are also positive and hence, there is a unique interior equilibrium if $A_0(r_0) > 0$.

Next assume that $A_0(r_0) < 0$ **and hence** $a_0(r_0) < 0$. In this case, since $A_2(r_0) > 0$, $\hat{P}(S) = 0$ has one positive solution and one negative solution and hence there is at most one interior equilibrium. Since $a_2(r_0) < 0$, both solutions of $P(C) = 0$ have the same sign or are complex. However, using similar reasoning as in the previous case, if both solutions of $P(C) = 0$ are negative or complex, substituting them into (42), it would imply that the two corresponding solutions of $\hat{P}(S) = 0$ are positive or complex, contradicting the fact that one is positive and one is negative. Hence, when $A_0(r_0) < 0$, both solutions of $P(C) = 0$ must be positive, and again there is a unique interior equilibrium.

Finally, assume $A_0(\widehat{r}_0) = 0$ **for some** $\widehat{r}_0 \in (r_0^c, r_0^b)$. If the degenerate case (35) holds, then by Lemma 7 *vi)* and *vii)* both $\hat{P}(S) = 0$ and $P(C) = 0$ are linear and each equation has a unique positive solution. Hence, there is a unique interior equilibrium. In the non-degenerate case, by Lemma 4, $\frac{dA_0(\widehat{r}_0)}{dr_0} \neq 0$. Therefore, there exists $\delta > 0$ such that $A_0(r_0) \neq 0$ for all $r_0 \in (\widehat{r}_0 - \delta, \widehat{r}_0) \cup (\widehat{r}_0, \widehat{r}_0 + \delta)$. If $(S(r_0), C(r_0))$ denotes the unique positive solution of $\hat{P}(S) = 0$ and $P(C) = 0$ for $r_0 \in (\widehat{r}_0 - \delta, \widehat{r}_0)$, then, since this solution is continuous in r_0, and since $\lim_{r_0 \to \widehat{r}_0} (S(r_0), C(r_0)) = (S(\widehat{r}_0), C(\widehat{r}_0))$ exists, $(S(\widehat{r}_0), C(\widehat{r}_0))$ is also a nonnegative solution of $\hat{P}(S) = 0$ and $P(C) = 0$. Since both equations are linear now, $(S(\widehat{r}_0), C(\widehat{r}_0))$ is the unique solution for $r_0 = \widehat{r}_0$. In fact, both $S(\widehat{r}_0)$ and $C(\widehat{r}_0)$ are positive because, otherwise, $S(\widehat{r}_0) = 0$ would imply that $\widehat{r}_0 = r_0^b$ and $C(\widehat{r}_0) = 0$ woud imply that $\widehat{r}_0 = r_0^c$, giving a contradiction in both cases. Thus, there is also a unique interior equilibrium when $A_0(r_0) = 0$.

Case (b).

Assume that $r_0 > \max\{r_0^c, r_0^b\}$. Then, by Lemma 3(a)*ii)*, $a_2(r_0) < 0$ and by Lemma 3 (b)*ii)* $A_2(r_0) < 0$. By Lemma 1, $\bar{r}_0 < r_0^c$ and so $B_c(r_0) < 0$, where B_c is the coefficient of S in (7), and is defined in (32).

First assume that $A_0(r_0) > 0$ and hence $a_0(r_0) > 0$. Since $A_2(r_0) < 0$, $\hat{P}(S) = 0$ defined in (5) is concave up with vertical intercept negative and so has one positive solution and one negative solution. Similarly, $P(C) = 0$ defined in (9), has one positive solution and one negative solution. On $(\max\{r_0^c, r_0^b\}, r_0^*)$, by Lemma 2, $B > 0$, and since the coefficient of S in (7), $B_c(r_0) < 0$, from (7), it follows that the negative solution of $\hat{P}(S) = 0$ corresponds to the positive solution of $P(C) = 0$, and hence the positive solution of $\hat{P}(S) = 0$ must correspond to the negative solution of $P(C) = 0$. Thus, there are no interior equilibria in this case. Also, if $r_0 \geq r_0^*$, then by Lemma 2, $B \leq 0$.

From the rearrangement of (7) given in (42), and noting the denominator is negative, again the negative solution of $P(C) = 0$ corresponds to the positive solution of $\hat{P}(S) = 0$, and hence there are no interior equilibria in this case.

Next assume that $A_0(r_0) < 0$ **and hence** $a_0(r_0) < 0$. Since, $A_2(r_0) < 0$, both roots of $\hat{P}(S) = 0$ defined in (5) have the same sign or they are both complex. As well, $a_2(r_0) < 0$, and so both roots of $\hat{P}(C) = 0$, defined in (9), have the same sign or they are both complex. If $r_0 \geq r_0^*$, then $B \leq 0$ and $B_c(r_0) < 0$, and so from (7) the two positive roots of $P(C) = 0$ correspond to two negative roots of $\hat{P}(S) = 0$, and hence there are no interior equilibria in this case. However, if $r_0 \in (\max\{r_0^c, r_0^b\}, r_0^*)$, then $B > 0$, and although it follows from (42), that the two negative roots of $P(C) = 0$ would correspond to the two positive roots of $\hat{P}(S) = 0$, we cannot rule out the possibility that the two positive roots of $P(C) = 0$ correspond to two positive roots of $\hat{P}(S) = 0$, and hence there can be at most two interior equilibria.

Finally, assume that there exists $\widehat{r_0}$ **such that** $A(\widehat{r_0}) = 0$. In the degenerate case, by Lemma 7 *viii)*, then the solution of at least one of the equations $\hat{P}(S) = 0$ or $P(C) = 0$ is not positive and hence there is no interior equilibrium. If the degenerate case (35) is not satisfied, then, $\hat{P}(S) = 0$ and $P(C) = 0$ are linear, and so there is at most one interior equilbrium. If $r_0 \geq r_0^*$, then $B \leq 0$ and $B_c(r_0) < 0$. Using (7), if the solution of $\hat{P}(S) = 0$ is positive, it follows that the corresponding value of C is negative, and hence there are no interior equilibria in this case. However, if there exists $\widehat{r_0} \in (\max\{r_0^c, r_0^b\}, r_0^*)$, we have $B(r_0) > 0$, so that even though $a_0(\widehat{r_0}) = 0$, and so by Lemma 4, $B_c(\widehat{r_0}) < 0$, we cannot rule out the possibility of a unique interior equilibrium.

Case (c). Assume $r_0 \in (r_0^b, r_0^c)$. Therefore, by Lemma 3(a)*i)*, $a_2(r_0) > 0$ and by Lemma 3(b) $r_0^b > \tilde{d}$ and (c)*ii)*, $A_2(r_0) < 0$. Also, by Lemma 1, $\bar{r}_0 < r_0^c$ and so $B_c(r_0) < 0$, where B_c is the coefficient of S in (7), and is defined in (32).

First assume that $A_0(r_0) > 0$ and so $a_0(r_0) > 0$. By $\hat{P}(S) = 0$ is a quadratic equation that is concave up and since $A_2(r_0) < 0$, the vertical intercept is negative. Therefore, $\hat{P}(S) = 0$ has one positive solution and one negative solution. Hence, there is at most one interior equilibrium. By (7), the corresponding C components are defined and real and by Lemma 2, since $r^* > r_0^c$, $B > 0$. Therefore, independent of the sign of the coefficient of S in (7), at least one of the C components is positive. Hence, the roots of $P(C) = 0$ defined in (9) must be real, and at least one is positive. Since the coefficient of $P(C) = 0$ in (9) are $a_0(r_0) > 0$ and $a_2(r_0) > 0$, the solutions of $P(C) = 0$ must have the same sign, and so they must both be positive. Therefore, the C component defined in (7) corresponding to the positive solution of $\hat{P}(S) = 0$, is also positive. By (8), the corresponding values of $E^\dagger$ and $V^\dagger$ are also positive and hence, there is a unique interior equilibrium if $A_0(r_0) > 0$.

Next assume that $A_0(r_0) < 0$ and hence $a_0(r_0) < 0$.

In this case, $P(C) = 0$ is concave down and since $a_0(r_0) > 0$, the vertical intercept is positive. Hence, there is one positive and one negative solution of $P(C) = 0$, and hence, at most one interior equilibrium. As well, $r_0 \in (\max\{r_0^b, \bar{r}_0\}, r_0^c)$, since if $r_0^b < r_0 \leq \bar{r}_0$, then by Lemma 1, $B_c(r_0) \geq 0$, contradicting $A_0(r_0) < 0$ and hence $B_c(r_0) < 0$ by Lemma 4. When, $A_0(r_0) < 0$ and $r_0 \in (\max\{r_0^b, \bar{r}_0\}, r_0^c)$. the denominator in (42) is negative, and by Lemma 2, $B > 0$. Therefore, the negative solution, C, of $P(C) = 0$ gives a positive value of S in (42). On the other hand, $A_0(r_0) < 0$ and $A_2(r_0) < 0$ and so both solutions of $\hat{P}(S) = 0$ must have the same

sign. Therefore, both corresponding values of S are positive, and once again there is a unique interior equilibrium when $A_0(r_0) < 0$.

Finally, assume that $A_0(\widehat{r}_0) = 0$ and hence $a_0(\widehat{r}_0) = 0$ for some $\widehat{r}_0 \in (r_0^b, r_0^c)$. If the degenerate case (35) holds, by Lemma 7 *vi)* and *vii)*, both $\hat{P}(S) = 0$ and $P(C) = 0$ have a unique positive solution and hence there is a unique interior equilibrium. Next consider the non-degenerate case. By Lemma 5, in the nondegenerate case $\frac{d\,A(\widehat{r}_0)}{d\,r_0} \neq 0$, and so the zero of $A_0(r_0)$ at $\widehat{r}_0$ is isolated, i.e., $\widehat{r}_0$ is the only point in (r_0^b, r_0^c) such that $A_0(r_0) = 0$. Note also that, $\widehat{r}_0 \neq \bar{r}_0$, since by Lemma 1, if $\bar{r}_0 > 0$ then $\tilde{d} > \alpha e^{\hat{d}\tau}$ and so $a_0(\bar{r}_0) = \frac{\alpha r \hat{d} \phi^2 (\tilde{d} - \alpha e^{-\hat{d}\tau})}{d} > 0$, contradicting $a_0(\widehat{r}_0) = 0$. By Lemma 4, since $A_0(\widehat{r}_0) = 0$, $B_c(r_0) < 0$ and therefore $r_0^c > \widehat{r}_0 > \bar{r}$. Since $A_0(\widehat{r}_0) = 0$, $\widehat{r}_0 \in (r_0^b, r_0^c)$, and $\widehat{r}_0 > \bar{r}$, there exists $\delta > 0$ such that $\widehat{r}_0 - \delta > \bar{r}_0$, $a_0(r_0) \neq 0$ for all $r_0 \in (\widehat{r}_0 - \delta, \widehat{r}_0) \cup (\widehat{r}_0, \widehat{r}_0 + \delta)$, and $B_c(r_0) < 0$. If $S(r_0)$ denotes the the unique positive solution of the $\hat{P}(S(r_0)) = 0$ with corresponding positive solution $C(r_0)$ of $P(C(r_0)) = 0$ on $(\widehat{r}_0 - \delta, \widehat{r}_0)$, just shown above to exist, then, since this solution is continuous in r_0, and since $\lim_{r_0 \to \widehat{r}_0} (S(r_0), C(r_0)) = (S(\widehat{r}_0), C(\widehat{r}_0))$ exists, $(S(\widehat{r}_0), C(\widehat{r}_0))$ is also a nonnegative solution of (5) and $P(C(\widehat{r}_0)) = 0$. Since both equations $\hat{P}(S) = 0$ and $P(C) = 0$ are linear, $(S(\widehat{r}_0), C(\widehat{r}_0))$ is the unique solution. In fact, both $S(\widehat{r}_0)$ and $C(\widehat{r}_0)$ are positive, because otherwise, if $S(\widehat{r}_0) = 0$ ($C(\widehat{r}_0) = 0$), that would mean $\widehat{r}_0 = r_0^b$ ($\widehat{r}_0 = r_0^c$), contradicting $\widehat{r} \in (r_0^b, r_0^c)$. Thus, we also have a unique interior equilibrium when $A_0(\widehat{r}_0) = 0$.

$\mathcal{E}_c$ exists provided $\tilde{d} < r_0$. Since $r_0^b - \tilde{d} = \frac{\tilde{d}\mu(r-d)}{d(K\phi\alpha d\mu)} > 0$, hence $\tilde{d} < r_0$ for all $r_0 \in [r_0^b, r_0^c]$ and therefore E_c exists for all $r_0 \in [r_0^b, r_0^c]$. The local stability of $\mathcal{E}_0$ follows from Theorem 1 and of $\mathcal{E}_c$ follows from Theorem 2.

Case (d). Assume that $0 < r_0 < \min\{r_0^c, r_0^b\}$.

Therefore, by Lemma 3 (a)*i)*, $a_2(r_0) > 0$ and by Lemma 3 (b) *i)*, $A_2(r_0) > 0$.

In case *i)*, since $A_0(r_0) > 0$ and hence $a_0(r_0) > 0$, therefore, both polynomials $\hat{P}(S) = 0$ and $P(C) = 0$ either have two positive roots or no positive roots, depending on the sign of $A_1(r_0)$.

Therefore, there can be 0, 1, or 2 interior equilibria, (one in the case of a double positive root, i.e., at a saddle-node bifurcation). See Fig. 1 b) for an example showing all three possibilities.

In case *ii)*, since $A_0(r_0) \leq 0$ and hence $a_0(r_0) \leq 0$, both polynomials $\hat{P}(S) = 0$ and $P(C) = 0$ either have no solution or have one positive solution and one negative solution, and hence there is at most one interior equilibrium. Since we are assuming that $A_0(r_0) \leq 0$, by Lemma 4, $B_c < 0$ where B_c is defined in (32). Therefore, by Lemma 1, $r_0 \in (\bar{r}_0, \min\{r_0^c, r_0^b\})$, by Lemma 2, since $\min\{r_0^c, r_0^b\}) < r^*$, we have $B > 0$. From (42), it follows that the negative root of $P(C) = 0$ corresponds to the positive root of $\hat{P}(S) = 0$ and from (7) it follows that the negative root of $\hat{P}(S) = 0$ corresponds to the postiive root of $P(C) = 0$. Hence, there are no interior equilibria in this case.

□

A.7 Proof of Theorem 6

To simplify the notation in system (1), we first use the dimensionless time, $\tilde{t} = \phi S_0 t$, and the dimensionless delay, $\tilde{\tau} = \phi S_0 \tau$, where $S_0 = K\left(1 - \frac{d}{r}\right)$. Then we rescale the variables of the model (1) by letting $s = \frac{S}{S_0}$, $\bar{e} = \frac{E}{S_0}$, $c = \frac{C}{S_0}$, $p = \frac{V}{S_0}$. In addition, in dimensionless form, the parameters are as follows: $r_1 = \frac{r-d}{\phi S_0}$, $r_2 = \frac{r_0 - \tilde{d}}{\phi S_0}$, $b = \frac{\alpha}{\phi S_0}$, $d_2 = \frac{\mu}{\phi S_0}$, $d_1 = \frac{\hat{d}}{\phi S_0}$, $a = \frac{S_0}{C_0}$, with $C_0 = K\left(1 - \frac{\tilde{d}}{r_0}\right)$. For rest of the paper, we will assume that $r > d$. Also notice that $r_2, a > 0$, whenever $r_0 > \tilde{d}$.
Now, for notational convenience, we replace $\tilde{t}$ and $\tilde{\tau}$ with t and τ, respectively, and obtain the following system:

$$\begin{aligned} s'(t) &= r_1 s(t)(1 - n(t)) - s(t)p(t) \\ \bar{e}'(t) &= s(t)p(t) - d_1\bar{e}(t) - e^{-d_1\tau}s(t-\tau)p(t-\tau) \\ c'(t) &= r_2 c(t)(1 - an(t)) + e^{-d_1\tau}s(t-\tau)p(t-\tau) \\ p'(t) &= bc(t) - s(t)p(t) - d_2 p(t), \end{aligned} \tag{43}$$

where $n = s + \bar{e} + c$.

We can write (43) in the form

$$x'(t) = f(x_t), \tag{44}$$

where $x = (s, \bar{e}, c, p)$ and $f \in C_+$ (recall that $C_+ := \{F : [-\tau, 0] \to \mathbb{R}^4_+ \mid F \text{ is continuous}\}$), where

$$f(\phi) = \begin{pmatrix} r_1\phi_1(0)[1 - (\phi_1(0) + \phi_2(0) + \phi_3(0))] - \phi_1(0)\phi_4(0) \\ \phi_1(0)\phi_4(0) - d_1\phi_2(0) - e^{-d_1\tau}\phi_1(-\tau)\phi_4(-\tau) \\ r_2\phi_3(0)(1 - a(\phi_1(0) + \phi_2(0) + \phi_3(0))) + e^{-d_1\tau}\phi_1(-\tau)\phi_4(-\tau) \\ b\phi_3(0) - \phi_1(0)\phi_4(0) - d_2\phi_4(0) \end{pmatrix} \tag{45}$$

In equation (44), by $x_t(\phi)$ we denote the member of C_+ that satisfies $x_t(\phi)(\theta) = x(t + \theta, \phi)$, where $x(t, \phi)$ is the solution of (43) that satisfies $x(\theta, \phi) = \phi(\theta)$ for all $\theta \in [-\tau, 0]$. From the theory of delay differential equations (see, e.g., Hale and Lunel 1993) it follows that (43) has a unique solution $x(t, \phi)$ that exists for all $t \geq 0$ and coincides with ϕ on the interval $[-\tau, 0]$. It is known that $(t, \phi) \mapsto x_t(\phi)$ is a continuous semiflow.

Let $D = \{\phi \in C_+ \mid \phi_2(0) = 0 \Rightarrow \phi_1(0)\phi_4(0) - e^{-d_1\tau}\phi_1(-\tau)\phi_4(-\tau) \geq 0\}$. Then, if $\phi \in D$ such that $\phi_i(0) = 0$, we have $f_i(\phi) \geq 0$. Further, from Theorem 2.1 in (Smith 1995), we have that any solution $x(t, \phi)$ of (43) with $\phi \in D$ is nonnegative for all $t \geq 0$. This further implies that D is positively invariant. Thus we consider the set D to be the state space for model (43).

The boundary equilibrium points of (43) are $\mathcal{E}_0^0 = (0, 0, 0, 0)$, $\tilde{\mathcal{E}}_0 = (1, 0, 0, 0)$ and $\tilde{\mathcal{E}}_c = (0, 0, 1/a, b/(d_2 a))$. Obviously, the stability properties of $\mathcal{E}_0^0$, $\tilde{\mathcal{E}}_0$ and $\tilde{\mathcal{E}}_c$ for system (43) are the same as those of $\mathcal{E}_0^0$, $\mathcal{E}_0$ and $\mathcal{E}_c$ for system (1), respectively.

Abusing notation, we also use $||\cdot||$ to denote the "*sup*" norm on a space $\{g : [-\tau, 0] \to \mathbb{R}_+^k \mid g \text{ is continuous}\}$. It will be clear from the context to which norm we will be referring.

Before we give of Theorem 6, we need a few preliminary results. We begin by establishing the existence of a compact attractor of bounded sets. Theorem 5 in Smith and Zhao (2001), which we use for the proof of our theorem, uses a slightly weaker assumption, namely the existence of a compact attractor of points. For mathematical completeness, we provide below the more general result.

Theorem 7 *There exists a unique global attractor of bounded sets corresponding to (44).*

Proof First, we show that $x_t(\phi)$ is point dissipative. Recall that $n(t) = s(t)+\bar{e}(t)+c(t)$. Then

$$n'(t) \leq r_1 s(t)(1 - n(t)) + r_2 c(t)(1 - an(t)) \tag{46}$$

Hence, the set $B_1 := \{x \in \mathbb{R}_+^4 \mid x_1 + x_2 + x_3 \leq \max\{1, 1/a\}\}$ attracts all solutions of (43), and no solution that enters B_1 can escape this set in forward time. Thus, there exists $K > 0$ such that, for all large t,

$$p'(t) \leq K - d_2 p(t) \tag{47}$$

From (46) and (47) we obtain that $x(t, \phi) = (s(t), \bar{e}(t), c(t), p(t)) \in B$ for all large t and all $\phi \in D$, where $B = \{x \in \mathbb{R}_+^4 \mid x_1 + x_2 + x_3 \leq 2\max\{1, 1/a\},\ x_4 \leq 2K/d_2\}$. Consequently (recall that $x_t(\phi)(\theta) = x(t + \theta, \phi)$), $x_t(\phi) \in \mathcal{B} := \{F \in D \mid F(\theta) \in B,\ \forall\, \theta \in [-\tau, 0]\}$ for all large t and all $\phi \in D$.

Next we show that $x_t(\phi)$ is asymptotically smooth. That is, for every positively invariant, bounded, closed set $S \subset D$, every sequence $x_{t_n}(\phi_n)$ with $t_n \to \infty$, $\phi_n \in S$, has a convergent subsequence. From (45) we see that f maps bounded sets in D to bounded sets in $\mathbb{R}^4$. Thus, there exists $k > 0$ such that $||f(\phi)|| \leq k$ for all $\phi \in S$. Further, we have

$$||x_{t_n}(\phi_n)(\tau_2) - x_{t_n}(\phi_n)(\tau_1)|| = \left|\left| \int_{t_n+\tau_1}^{t_n+\tau_2} f(x_l)\, dl \right|\right| \leq k|\tau_2 - \tau_1|$$

Hence, from the Arzela-Ascoli theorem, the set $\{x_{t_n}(\phi_n) \mid n \geq 0\}$ is precompact and so it has a convergent subsequence.

Finally, we show that (44) is eventually bounded on every bounded set. Thus, let R be a bounded set in D. Let $n_{max} \geq \max\{1, 1/a, \sup_{\phi \in R} ||\phi_1|| + ||\phi_2|| + ||\phi_3||\}$ and $p_{max} \geq \max\{K/d_2, \sup_{\phi \in R} ||\phi_4||\}$. Then, using (46) and (47), we have that the set $R_B := \{\phi \in D \mid ||\phi_1|| + ||\phi_2|| + ||\phi_3|| \leq n_{max},\ ||\phi_4|| \leq p_{max}\}$ is bounded, positively invariant and contains R.

Now the conclusion follows from Theorem 2.33 in (Smith and Thieme 2011).

□

Consider the nonautonomous linear systems

$$u^{1'}(t) = A_1(x_t(\phi))u^1(t), \tag{48}$$
$$u^{2'}(t) = A_2(x_t(\phi))u^2(t) + B_2(x_t(\phi))u^2(t-\tau), \tag{49}$$

where

$$A_1(x_t(\phi)) = r_1[1 - n_t(\phi)(0)] - p_t(\phi)(0), \tag{50}$$
$$A_2(x_t(\phi)) = \begin{pmatrix} r_2(1 - an_t(\phi)(0)) & 0 \\ b & -(d_2 + s_t(\phi)(0)) \end{pmatrix}, \tag{51}$$
$$B_2(x_t(\phi)) = \begin{pmatrix} 0 & e^{-d_1\tau}s_t(\phi)(-\tau) \\ 0 & 0 \end{pmatrix} \tag{52}$$

Denote by $L_i(t,\phi)$, $i = 1, 2$, the solution operators for (48) and (49), respectively. Thus, $L_1(t,\phi) : \mathbb{R}_+ \to \mathbb{R}_+$, $L_1(t,\phi)\eta = u^1(t,\eta,\phi)$, and $L_2(t,\phi) : C_+^2 \to C_+^2$, $L_2(t,\phi)\eta = u_t^2(\eta,\phi)$, where $C_+^2 = \{F : [-\tau, 0] \to \mathbb{R}_+^2 \mid F \text{ is continuous}\}$. Also, $L_i(0,\phi)\eta = \eta$, for all $\phi \in D$, $\eta \in C_+^i$, where, for convenience, we write C_+^1 for $\mathbb{R}_+$. Then we have that

$$L_i(t_2, x_{t_1}(\phi))L_i(t_1,\phi)\eta = L_i(t_1+t_2,\phi)\eta,\ \forall\, t_1 \geq 0,\ t_1+t_2 \geq 0,\ \phi \in D,\ \eta \in C_+^i \tag{53}$$

We define $||L_2(t,\phi)|| = \sup\{||L_2(t,\phi)\eta|| \mid \eta \in C_+^2,\ ||\eta|| = 1\}$. For $\phi \in C_+$ and $\eta > 0$, let

$$\lambda_i(\phi,\eta) = \limsup_{t\to\infty} \frac{1}{t} \ln ||L_i(t,\phi)\eta||,\ i = 1, 2. \tag{54}$$

The following notation (borrowed from Smith 1995) will prove useful. Thus, for $\eta \in C_+^2$, $\eta \gg 0$ means $\eta_i(\theta) > 0$, $\forall\, i = 1, 2$, $\forall\theta \in [-\tau, 0]$, while $\eta > 0$ means $\exists\,\theta \in [-\tau, 0]$, $\exists\, i = 1, 2$ such that $\eta_i(\theta) > 0$.

Lemma 8 *$\lambda_2(\tilde{\mathcal{E}}_0,\eta) = \lambda_2(\tilde{\mathcal{E}}_0,\xi)$, for all $\eta, \xi > 0$.*

Proof Equation (49) can be written as

$$u^{2'}(t) = Pu_t^2, \tag{55}$$

where, for $\eta \in C_+^2$, $P\eta = A_2(x_t(\tilde{\mathcal{E}}_0))\eta(0) + B_2(\tilde{\mathcal{E}}_0)\eta(-\tau)$.

For every $\eta \in C_+^2$, $\eta_1(0) = 0$ implies $P_1(t)\eta = e^{-d_1\tau}\eta_2(-\tau) \geq 0$, while $\eta_2(0) = 0$ implies $P_2(t)\eta = b\eta_1(0)) \geq 0$. Thus, (49) is cooperative.

For $j = 1, 2$, let $\hat{e}^j \in C_+^2$ be defined as $\hat{e}_k^j(t) = \delta_{jk}$ (the Kronecker delta), for all $t \in [-\tau, 0]$. Then

$$col(P\hat{e}^1, P\hat{e}^2) = \begin{pmatrix} r_2(1-a) & e^{-d_1\tau} \\ b & -(d_2+1) \end{pmatrix}$$

is an irreducible matrix. Thus, (48) is cooperative and irreducible in $C_+^2 \setminus \{0\}$.

Also, we can write $P_j\eta$, $j = 1, 2$, as

$$P_j\eta = a_j\eta_j(0) + \sum_{k=1}^{2} \int_{-\tau_k}^{0} \eta_k(\theta) d_\theta \nu_{jk}(t, \theta),$$

where $\tau_1 = 0$, $\tau_2 = \tau$, $a_1 = r_2(1-a)$, $a_2(t) = -(d_2+1)$, $\nu_{11} = \nu_{22} = 0$ (the zero measure), $\nu_{12}(t, \theta) = e^{-d_1\tau}\delta_{-\tau}$, and $\nu_{21} = b\delta_0$, where δ_θ is the Dirac measure based at θ.

From Lemma 3.2 in Smith (1995) (note that condition (R) on p.86 is satisfied), we obtain that if $u^2(t, \eta)$ is a solution of (49) with $\eta > 0$ then $u^2(t, \eta) \gg 0$ for all $t \geq 2\tau$.

Now let $\eta, \xi \gg 0$. That is, $\eta_i(\theta),\ \xi_i(\theta) > 0$, for all $\theta \in [-\tau, 0]$, $i = 1, 2$. Then there exist $a, b > 0$ such that $a\eta \leq \xi \leq b\eta$. From (54) and the fact that (49) is cooperative, we obtain $\lambda_2(\phi, \eta) = \lambda_2(\phi, \xi)$.

Let $\eta \in C_+^2$, $\eta > 0$. Let $\xi = L_2(2\tau, \phi)\eta$.Then

$$\begin{aligned}
\lambda_2(\phi, \eta) &= \limsup_{t\to\infty} \frac{1}{t} \ln ||L_2(t, \phi)\eta|| \\
&= \limsup_{t\to\infty} \frac{1}{t} \ln ||L_2(t-2\tau, x_{2\tau}(\phi))L_2(2\tau, \phi)\eta|| \\
&= \limsup_{t\to\infty} \frac{t-2\tau}{t} \cdot \frac{1}{t-2\tau} \ln ||L_2(t-2\tau, x_{2\tau}(\phi))\xi|| \\
&= \limsup_{t\to\infty} \frac{1}{t} \ln ||L_2(t, x_{2\tau}(\phi))\xi|| \\
&= \lambda_2(x_{2\tau}(\phi), \xi) \\
&= \lambda_2(x_{2\tau}(\phi), L_2(2\tau, \phi)\xi) \\
&= \limsup_{t\to\infty} \frac{1}{t} \ln ||L_2(t, x_{2\tau}(\phi))L_2(2\tau, \phi)\xi|| \\
&= \limsup_{t\to\infty} \frac{1}{t} \ln ||L_2(t+2\tau, \phi)\xi|| \\
&= \limsup_{t\to\infty} \frac{t+2\tau}{t} \frac{1}{t+2\tau} \ln ||L_2(t+2\tau, \phi)\xi|| \\
&= \limsup_{t\to\infty} \frac{1}{t} \ln ||L_2(t, \phi)\xi|| \\
&= \lambda_2(\phi, \xi)
\end{aligned}$$

□

Thus, in what follows we will often write, in short, $\lambda(\phi)$ for $\lambda(\phi, \eta)$.

Lemma 9 *There exist $\delta > 0$ and a neighborhood V of $\tilde{\mathcal{E}}_0$ such that the set*

$$U_2 := \left\{ \frac{L_2(t+\tau,\phi,\gamma)\eta}{||L_2(t,\phi,\gamma)\eta||} \mid t \geq 0,\ \eta \in C_+^2 \setminus \{0\},\ ||\gamma - \gamma_0|| < \delta,\ x_T(\phi,\gamma) \in V,\ \forall\, T \geq 0 \right\} \quad (56)$$

is precompact and its closure is contained in $C_+^2 \setminus \{0\}$.

Proof There exists V' a neighborhood of $\tilde{\mathcal{E}}_0$ and $\kappa_1 > 0$ such that $||A_2(\phi)|| \leq \kappa_1$, $||B_2(\phi)|| \leq \kappa_1$, for all $\phi \in V'$. First, we show that the following set is precompact

$$U_2' := \left\{ \frac{L_2(t+\tau,\phi,\gamma)\eta}{||L_2(t,\phi,\gamma)\eta||} \mid t \geq 0,\ \eta \in C_+^2 \setminus \{0\},\ x_T(\phi,\gamma) \in V',\ \forall\, T \geq 0 \right\} \quad (57)$$

Let $L_2(t+\tau,\phi,\gamma)\eta/||L_2(t,\phi,\gamma)\eta|| \in U_2'$. Then $L_2(t+\tau,\phi,\gamma)\eta/||L_2(t,\phi,\gamma)\eta|| = L_2(\tau,\psi,\gamma)\xi$, where $\psi = x_t(\phi,\gamma)$ and $\xi = L_2(t,\phi,\gamma)\eta/||L_2(t,\phi,\gamma)\eta||$. From (49), we have

$$\begin{aligned}
L_2(\tau,\psi,\gamma)\xi(\theta) &= u_\tau^2(\xi,\psi,\gamma)(\theta) \\
&= u^2(\tau+\theta,\xi,\psi,\gamma) \\
&= \xi(0) + \int_0^{\tau+\theta} A_2(x_s(\psi,\gamma))u^2(s,\xi,\psi,\gamma)\,ds \\
&\quad + \int_0^{\tau+\theta} B_2(x_s(\psi,\gamma))u^2(s-\tau,\xi,\psi,\gamma)\,ds \\
&= \xi(0) + \int_{-\theta}^{\tau} A_2(x_{s+\theta}(\psi,\gamma))u^2(s+\theta,\xi,\psi,\gamma)\,ds \\
&\quad + \int_0^{\tau+\theta} B_2(x_s(\psi,\gamma))\xi(s-\tau)\,ds \\
||L_2(\tau,\psi,\gamma)\xi(\theta)|| &\leq 1 + \kappa_1\tau + \kappa_1 \int_{-\theta}^{\tau} ||L_2(s,\psi,\gamma)\xi(\theta)||\,ds \\
||L_2(\tau,\psi,\gamma)\xi(\theta)|| &\leq (1+\kappa_1\tau)e^{\kappa_1\tau}, \qquad (58)
\end{aligned}$$

where the last inequality follows from Gronwall's inequality. Thus, there exists $\kappa_2 > 0$ such that $||L_2(\tau,\psi,\gamma)|| \leq \kappa_2$, for all $\psi \in V'$, $\gamma \in \Gamma$.

Next we show that $\forall\, \varepsilon > 0$, $\exists\, \delta > 0$ such that, $\forall\, \theta_1, \theta_2 \in [-\tau, 0]$, $|\theta_2 - \theta_1| < \delta$, $\forall\, L_2(t+\tau,\phi,\gamma)\eta/||L_2(t,\phi,\gamma)\eta|| \in U_2'$, there holds

$$\frac{||L_2(t+\tau,\phi)\eta(\theta_2) - L_2(t+\tau,\phi)\eta(\theta_1)||}{||L_2(t,\phi,\gamma)\eta||} < \varepsilon \quad (59)$$

Again, from (49), we obtain that, for all $t \geq 0$,

$$L_2(t+\tau,\phi,\gamma)\eta(\theta) = u_{t+\tau}^2(\eta,\phi,\gamma)(\theta)$$

$$
\begin{aligned}
&= u^2(t+\tau+\theta,\eta,\phi,\gamma)\\
&= \eta(0) + \int_0^{t+\tau+\theta} A_2(x_s(\phi,\gamma))u^2(s,\eta,\phi,\gamma)\,ds\\
&\quad + \int_0^{t+\tau+\theta} B_2(x_s(\phi,\gamma))u^2(s-\tau,\eta,\phi,\gamma)\,ds.
\end{aligned}
$$

Thus, w.l.o.g assuming $\theta_1 < \theta_2$, we have

$$
\begin{aligned}
&||L_2(t+\tau,\phi,\gamma)\eta(\theta_2) - L_2(t+\tau,\phi,\gamma)\eta(\theta_1)||\\
&\le \int_{t+\tau+\theta_1}^{t+\tau+\theta_2} ||A_2(x_s(\phi,\gamma))||||u^2(s,\eta,\phi,\gamma)||\,ds\\
&\quad + \int_{t+\tau+\theta_1}^{t+\tau+\theta_2} ||B_2(x_s(\phi,\gamma))||||u^2(s-\tau,\eta,\phi,\gamma)||\,ds\\
&\le \kappa_1\Big(\int_{t+\tau+\theta_1}^{t+\tau+\theta_2} ||u^2(s,\eta,\phi,\gamma)||\,ds\\
&\quad + \int_{t+\tau+\theta_1}^{t+\tau+\theta_2} ||u^2(s-\tau,\eta,\phi,\gamma)||\,ds\Big)\\
&= \kappa_1\left(\int_{\theta_1}^{\theta_2} ||u^2(t+\tau+s,\eta,\phi,\gamma)||\,ds\right.\\
&\quad \left. + \int_{\theta_1}^{\theta_2} ||u^2(t+s,\eta,\phi,\gamma)||\,ds\right)\\
&= \kappa_1\left(\int_{\theta_1}^{\theta_2} ||u^2_{t+\tau}(\eta,\phi,\gamma)(s)||\,ds\right.\\
&\quad \left. + \int_{\theta_1}^{\theta_2} ||u^2_t(\eta,\phi,\gamma)(s)||\,ds\right)\\
&\le \kappa_1(\theta_2-\theta_1)(||u^2_{t+\tau}(\eta,\phi,\gamma)|| + ||u^2_t(\eta,\phi,\gamma)||)
\end{aligned}
$$

Hence

$$
\begin{aligned}
&\frac{||L_2(t+\tau,\phi,\gamma)\eta(\theta_2) - L_2(t+\tau,\phi,\gamma)\eta(\theta_1)||}{||L_2(t,\phi,\gamma)\eta||}\\
&\le \kappa_1(\theta_2-\theta_1)\left(1 + \frac{||u^2_{t+\tau}(\eta,\phi,\gamma)||}{||u^2_t(\eta,\phi,\gamma)||}\right)
\end{aligned}
\tag{60}
$$

On the other hand, using (53) have that

$$
\begin{aligned}
u^2_{t+\tau}(\eta,\phi,\gamma) &= L_2(\tau,x_t(\phi,\gamma),\gamma)L_2(t,\phi,\gamma)\eta\\
&= L_2(\tau,x_t(\phi,\gamma),\gamma)u^2_t(\eta,\phi,\gamma),\ \forall\, t \ge 0,
\end{aligned}
\tag{61}
$$

from which we obtain

$$||u^2_{t+\tau}(\eta,\phi,\gamma)|| \leq ||L_2(\tau, x_t(\phi,\gamma),\gamma)||||u^2_t(\eta,\phi,\gamma)|| \leq \kappa_2||u^2_t(\eta,\phi,\gamma)||, \quad (62)$$

Then (59) follows from (60) and (62).

Now from (59) and (62) we obtain, applying the Arzela-Ascoli theorem, that U_2' is precompact.

For $\delta > 0$ and $V \subset V'$ a neighborhood of $\tilde{\mathcal{E}}_0$, $U_2 \subset U_2'$, so U_2 is also precompact.

Suppose that for every $\delta > 0$ and every V a neighborhood of $\tilde{\mathcal{E}}_0$, the closure of the corresponding set U_2 is not contained in $C^2_+ \setminus \{0\}$. Then there exist sequences $(t_n)_n$, $(\phi_n)_n \subset C_+$, $\gamma_n \to \gamma_0$ and $(\eta_n)_n \subset C^2_+ \setminus \{0\}$, $x_{t_n}(\phi_n,\gamma_n) \to \tilde{\mathcal{E}}_0$, such that $L_2(\tau, x_{t_n}(\phi_n,\gamma_n),\gamma_n)\xi_n \to 0$, where $\xi_n = L_2(t_n,\phi_n,\gamma_n)\eta_n/||L_2(t_n,\phi_n,\gamma_n)\eta_n||$. For each n let θ_n be such that $||\xi_n(\theta_n)|| = 1$. For all large n, the differential equation

$$v'(t) = A_2(x_{t+\theta_n+t_n}(\phi_n,\gamma_n))v(t) + B_2(x_{t+\theta_n+t_n}(\phi_n,\gamma_n))v(t-\tau) \quad (63)$$

is satisfied by $L_2(t, x_{t_n}(\phi_n,\gamma_n),\gamma_n)\xi_n(\theta_n)$, for all $t > 0$. Consider the ordinary differential equation

$$w'(t) = A_2(x_{t+\theta_n+t_n}(\phi_n,\gamma_n))w(t) \quad (64)$$

Since matrix A_2 is quasipositive and matrix B_2 is nonnegative, we have that $L_2(t, x_{t_n}(\phi_n,\gamma_n),\gamma_n)\xi_n(\theta_n) \geq w_n(t) \geq 0$, $\forall\, t \geq 0$, for every solution $w_n(t)$ of (64) with $w_n(0) = \xi_n(\theta_n)$. Hence $w_n(\tau) = w(\tau, x_{t_n}(\phi_n,\gamma_n),\xi_n(\theta_n)) \to 0$ (where $x_{t_n}(\phi_n,\gamma_n)$ is regarded as a parameter for the solution w). There exists a subsequence $n_k \to \infty$ such that $\xi_{n_k}(\theta_{n_k}) \to \bar{\xi} \in \mathbb{R}^2_+$. Then $w(\tau,\tilde{\mathcal{E}}_0,\bar{\xi}) = 0$ and $||\bar{\xi}|| = 1$. By the uniqueness of solutions of (64), $\bar{\xi} = 0$, which represents a contradiction. This concludes our proof.

□

Lemma 10 *The set $\cup_{\phi\in D,\gamma\in\Gamma}\omega_\gamma(\phi)$ is precompact.*

Proof Let $\mathcal{A}_\Gamma = \cup_{\phi\in D,\gamma\in\Gamma}\omega_\gamma(\phi)$ and let $\psi \in \mathcal{A}_\Gamma$. Let $\varepsilon > 0$. Then there exists $\gamma \in \Gamma$, $\bar{\phi} \in D$ such that $d(\psi,\omega_\gamma(\bar{\phi})) < \varepsilon$ (where $d(\psi,\omega_\gamma(\bar{\phi}))$ denotes the distance between ψ and the set $\omega_\gamma(\bar{\phi})$). $\omega_\gamma(\bar{\phi})$ being compact, there exists $\psi_0 \in \omega_\gamma(\bar{\phi})$ such that $d(\psi,\omega_\gamma(\bar{\phi})) = d(\psi,\psi_0) = ||\psi-\psi_0||$. Also, $\omega_\gamma(\bar{\phi})$ being invariant, there exists $\phi_0 \in \omega_\gamma(\bar{\phi})$ such that $\psi_0 = x_\tau(\phi_0,\gamma)$. The system (43) can be written in the form $x'(t) = A(x_t)x(t) + B(x_t)x(t-\tau)$, with

$$A(\phi) = \begin{pmatrix} r_1[1-\sum_{i=1}^3\phi^i(0)] - \phi^4(0) & 0 & 0 & 0 \\ \phi^4(0) & -d_1 & 0 & 0 \\ 0 & 0 & r_2[1-a\sum_{i=1}^3\phi^i(0)] & 0 \\ 0 & 0 & b & -\phi^1(0)-d_2 \end{pmatrix} \quad (65)$$

$$B(\phi) = \begin{pmatrix} 0\,0\,0 & 0 \\ 0\,0\,0 & -e^{-d_1\tau}\phi^1(-\tau) \\ 0\,0\,0 & e^{-d_1\tau}\phi^1(-\tau) \\ 0\,0\,0 & 0 \end{pmatrix} \quad (66)$$

Let $\mathcal{B}(\gamma)$ be the set $\mathcal{B}$, defined in Theorem 7, corresponding to the parameter $\gamma \in \Gamma$. Then, since Γ is compact, $\cup_{\gamma\in\Gamma}\mathcal{B}(\gamma)$ is bounded. Therefore $\mathcal{A}_\Gamma$ is bounded (because $\omega_\gamma(\phi) \in \mathcal{B}(\gamma)$). Now using (65) and (66), we obtain that there exists $\kappa > 0$ such that $||\phi||, ||A(\phi)||, ||B(\phi)|| \leq \kappa$, for all $\phi \in \mathcal{A}_\Gamma$. Let $\theta_1, \theta_2 \in [-\tau, 0]$, $\theta_1 \leq \theta_2$. We have

$$\begin{aligned}
||\psi(\theta_2) - \psi(\theta_2)|| &\leq ||x(\tau+\theta_2, \phi_0, \gamma) - x(\tau+\theta_1, \phi_0, \gamma)|| + \\
&\quad + ||\psi(\theta_1) - x_\tau(\phi_0, \gamma)(\theta_1)|| + ||\psi(\theta_2) - x_\tau(\phi_0, \gamma)(\theta_2)|| \\
&\leq 2\varepsilon + \int_{\tau+\theta_1}^{\tau+\theta_2} ||A(x_s(\phi, \gamma))||||x(s, \phi, \gamma)||\, ds + \\
&\quad \int_{\tau+\theta_1}^{\tau+\theta_2} ||B(x_s(\phi, \gamma))||||x(s-\tau, \phi, \gamma)||\, ds \\
&\leq 2\varepsilon + \kappa\left(\int_{\tau+\theta_1}^{\tau+\theta_2} ||x(s, \phi, \gamma)||\, ds + \int_{\tau+\theta_1}^{\tau+\theta_2} ||\phi(s)||\, ds\right) \\
&= 2\varepsilon + \kappa^2(\theta_2 - \theta_1)
\end{aligned}$$

Then, from the Arzela-Ascoli theorem, we obtain that $\cup_{\phi\in D, \gamma\in\Gamma}\omega_\gamma(\phi)$ is precompact. □

Proof of Theorem 6 We will work here with the rescaled model (43) and apply Theorem 5 in Smith and Zhao (2001). Using Lemma 10, for each of the cases *i)-iv)* above we only need to verify the assumptions (**B1**) and (**B2**) of this theorem.

Let $X_0^1 = \{\phi \in D \mid \phi_1(0) = 0\}$, $X_0^2 = \{\phi \in D \mid \phi_3 = \phi_4 = 0\}$, and $X_0 = \{\phi \in D \mid \phi_1(0) = \phi_3(0) = 0\}$. Notice that all solutions originating in one of these sets remains in that set for all $t > 0$.

(i). It is trivial to verify that all solutions originating in X_0 converge to $\mathcal{E}_0^0 = (0, 0, 0, 0)$. We choose the "generalized distance function" from Theorem 5 in Smith and Zhao (2001) to be $\tilde{p}(\phi) = \phi_1(0) + \phi_3(0)$. Next we verify condition **(B2)** of this theorem for $\mathcal{E}_0^0$, arguing by contradiction. Thus, suppose $\forall\, \epsilon > 0, \delta_0 > 0, \exists\, \bar{\gamma}$, $||\bar{\gamma} - \gamma_0|| < \delta_0$, and $\bar{\phi} \in C_+ \setminus X_0$, such that

$$d(x_t(\bar{\phi}, \bar{\gamma}), \mathcal{E}_0^0) \leq \epsilon,\ \forall\, t \geq 0. \tag{67}$$

First assume that $\bar{\phi}_1(0) > 0$. From (43), $s(t) = s(t, \bar{\phi})$ satisfies

$$s'(t) = s(t)[r_1(1 - s(t) - \bar{e}(t)) - p(t)] \tag{68}$$

Hence, using (67) , we see that (for ϵ small) s would be increasing, thus convergent to a positive value, which would represent a contradiction.

Now assume that $\bar{\phi}_1(0) = 0$. Then $\phi_1(t) = s(t) = 0$ for all $t \geq 0$. Also, $\phi_3(0) > 0$, and $c(t)$ satisfies

$$c'(t) \geq r_2 c(t)[1 - a(\bar{e}(t) + c(t))],\ \forall\, t \geq 0$$

Since $\bar{e}(t) \to 0$ as $t \to \infty$, and since $c'(t) > 0$ if $c(t) < 1/(2a)$ for all large t, again we arrive to a contradiction to (67).

Assumption (**B1**) is satisfied by Theorem 7 and $\{\mathcal{E}_0^0\}$ being the only invariant set in X_0 and asymptotically stable (hence isolated and acyclic) in X_0. This concludes of this part.

For the remainder of we will assume, without a loss of generality, that the state space is disjoint from a certain neighborhood of $\mathcal{E}_0^0$.

(ii). All solutions originating in X_0^1 converge to $\tilde{\mathcal{E}}_c = (0, 0, 1/a, b/(d_2 a))$. We choose $\tilde{p}(\phi) = \phi_1(0)$. Next we verify condition **(B2)**, arguing by contradiction. Thus, suppose $\forall\, \epsilon > 0$, $\delta_0 > 0$, $\exists\, \bar{\gamma}$, $||\bar{\gamma} - \gamma_0|| < \delta_0$, and $\bar{\phi} \in C_+ \setminus X_0^1$, such that

$$d(x_t(\bar{\phi}, \bar{\gamma}), \tilde{\mathcal{E}}_c) \leq \epsilon,\ \forall\, t \geq 0. \tag{69}$$

We have $\lambda_1(\tilde{\mathcal{E}}_c) = r_1(1 - 1/a) - b/(d_2 a)$, which is positive, because $\mathcal{R}_S^{C_0} > 1$. Then it follows that tere exist $c > 1$, $T, \delta > 0$, and V_0 a bounded neighborhood of $\tilde{\mathcal{E}}_c$ such that

$$\forall\, \phi \in V_0,\ ||\gamma - \gamma_0|| < \delta, L_1(T, \phi, \gamma)1 > c \tag{70}$$

Assume that $\delta_0 < \delta$ and that ϵ is so small, so that $x_t(\bar{\phi}, \bar{\gamma}) \in V_0$, for all $t \geq 0$.

Notice that $L_1(t, \phi, \gamma)\phi_1(0) = s(t, \phi, \gamma)$. Applying (70) with γ replaced by $\bar{\gamma}$, ϕ replaced by $\bar{\phi}$ and 1 replaced by $\bar{\phi}_1(0)/\bar{\phi}_1(0)$ we obtain

$$s(T, \bar{\phi}, \bar{\gamma}) > c\bar{\phi}_1(0) \tag{71}$$

Next we apply again (70), this time with ϕ replaced by $x_T(\bar{\phi}, \bar{\gamma})$ and η replaced by $L_1(T, \bar{\phi}, \bar{\gamma})\bar{\phi}_1(0)/L_1(T, \bar{\phi}, \bar{\gamma})\bar{\phi}_1(0)$ and obtain (see (53))

$$s(2T, \bar{\phi}, \bar{\gamma}) > c^2\bar{\phi}_1(0) \tag{72}$$

By continuing this algorithm, we obtain that

$$s(nT, \bar{\phi}, \bar{\gamma}) > c^n\bar{\phi}_1(0),\ \forall\, n \geq 1 \tag{73}$$

This contradicts that $x_t(\bar{\phi}, \bar{\gamma}) \in V_0$, for all $t \geq 0$.

Assumption (**B1**) is satisfied by Theorem 7 and $\{\tilde{\mathcal{E}}_c\}$ being the only invariant set in X_0^1 and asymptotically stable (hence isolated and acyclic) in X_0^1. This concludes of this part.

(iii). On the set X_0^2 the equilibrium $\tilde{\mathcal{E}}_0$ is globally asymptotically stable, and so it is isolated and acyclic.

Next we calculate the Lyapunov exponent corresponding to $\tilde{\mathcal{E}}_0$. The characteristic equation associated with the linear, autonomous DDE (49), where $\phi = \tilde{\mathcal{E}}_0$, is

$$\lambda^2 - [r_2(1 - a) - (1 + d_2)]\lambda - r_2(1 - a)(1 + d_2) = be^{-(\lambda + d_1)\tau} \tag{74}$$

Further, $\mathcal{R}_0 > 1$ implies that (74) has a positive solution $\bar{\lambda}$. A corresponding eigenvector would be $\psi \in C^2$, $\psi(t) = e^{\bar{\lambda}t}v$, where $v \in \mathbb{R}^2 \setminus \{0\}$. Since

$$\begin{pmatrix} \bar{\lambda} - r_2(1-a) & -e^{-(\bar{\lambda}+d_1)\tau} \\ -b & \bar{\lambda} + (1+d_2) \end{pmatrix} \begin{pmatrix} v_1 \\ v_2 \end{pmatrix} = 0, \tag{75}$$

we can choose $v \in int(\mathbb{R}^2_+)$. Hence $\psi \gg 0$. From this it follows that $W^U(0)$, the unstable manifold of 0 for (49), contains points in $C^2_+ \setminus \{0\}$. Let $\xi \in (C^2_+ \setminus \{0\}) \cap W^U(0)$. Then $u(t, \xi)$, the solution of (48) with initial condition ξ does not converge to 0 as $t \to \infty$.

On the other hand, from Theorem 1.2 in Pituk (2018), $\lambda_2(\tilde{\mathcal{E}}_0) = \lambda_2(\tilde{\mathcal{E}}_0, \xi) = \lim_{t\to\infty}(1/t)\ln||u_t(\xi)||$ is a real root μ of (74) associated with an eigenvector in C^2_+. Hence (75) is satisfied with $\bar{\lambda}$ replaced by μ and with v replaced by some $u \in int(\mathbb{R}^2_+)$.

Suppose that $\mu < 0$. Then, from (75) it follows that $\mu > \max\{-(1+d_2), -r_2(a-1)\}$, which leads to a contradiction to μ being a real solution to (74), because $be^{-d_1\tau} > r_2(a-1)(1+d_2)$. Hence $\mu > 0$.

Next we verify condition **(B2)** of Theorem 5 in Smith and Zhao (2001) for $\tilde{\mathcal{E}}_0$. For convenience, for a $\phi \in C_+$ we denote (ϕ_3, ϕ_4) by ϕ^2. Thus, we show that $\exists \epsilon_2, \delta_2 > 0$, such that

$$\limsup_{t\to\infty} d(x_t(\phi, \gamma), \tilde{\mathcal{E}}_0) > \epsilon_2, \ \forall\, \phi \in D, \ ||\phi^2|| > 0, \ ||\gamma - \gamma_0|| < \delta_2 \tag{76}$$

We prove this arguing by contradiction. Thus, suppose $\forall \epsilon_2, \delta_2 > 0, \exists \bar{\gamma}, ||\gamma - \gamma_0|| < \delta_2$, and $\bar{\phi} \in C_+, \ ||\bar{\phi}^2|| > 0$, such that

$$d(x_t(\bar{\phi}, \bar{\gamma}), \tilde{\mathcal{E}}_0) \le \epsilon_2, \ \forall\, t \ge 0. \tag{77}$$

Since $\lambda_2(\tilde{\mathcal{E}}_0) > 0$, we have $\lambda_2(\tilde{\mathcal{E}}_0, \eta) > 0$ for all $\eta \in \bar{U}_2$ (see Lemma 8). Further, using that U_2 (for some δ and V) is precompact and $\bar{U}_2 \subset C^2_+ \setminus \{0\}$ (Lemma 9), it follows that there exist $c > 1$, $T_1, \ldots, T_k, \delta_1 \in (0, \delta)$, and $V_2 \subset V$ a bounded neighborhood of $\tilde{\mathcal{E}}_0$ such that

$$\forall\, \phi \in V_2, \ \eta \in U_2, \ ||\gamma - \gamma_0|| < \delta_1, \ \exists\, j \in \{1, \ldots, k\} \text{ such that } ||L_2(T_j, \phi, \gamma)\eta|| > c||\eta|| \tag{78}$$

Assume that $\delta_2 < \delta_1$ and that ϵ_2 is so small, so that $x_t(\bar{\phi}, \bar{\gamma}) \in V_2$, for all $t \ge 0$.

Notice that $L_2(t, \phi, \gamma)\phi^2 = x^2_t(\phi, \gamma)$. Applying (78) with γ replaced by $\bar{\gamma}$, ϕ replaced by $x_\tau(\bar{\phi}, \bar{\gamma})$ and η replaced by $L_2(\tau, \bar{\phi}, \bar{\gamma})\bar{\phi}^2/||\bar{\phi}^2||$ we obtain

$$||x^2_{T_{j_1}+\tau}(\bar{\phi}, \bar{\gamma})|| > c||\bar{\phi}^2||, \tag{79}$$

for some $T_{j_1} \in \{T_1, ..., T_k\}$. Next we apply again (78), this time with ϕ replaced by $x_{T_{j_1}+2\tau}(\bar{\phi}, \bar{\gamma})$ and η replaced by $L_2(T_{j_1} + 2\tau, \bar{\phi}, \bar{\gamma})\bar{\phi}^2/||L_2(T_{j_1} + \tau, \bar{\phi}, \bar{\gamma})\bar{\phi}^2||$ we obtain

$$||x^2_{T_{j_1}+T_{j_2}+2\tau}(\bar{\phi}, \bar{\gamma})|| > c^2||\bar{\phi}^2||, \tag{80}$$

for some $T_{j_2} \in \{T_1, ..., T_k\}$. By continuing this algorithm, we obtain that

$$||x^2_{t_n}(\bar{\phi}, \bar{\gamma})|| > c^n ||\bar{\phi}^2||, \tag{81}$$

where, for arbitrarily large n, $t_n = \sum_{m=1}^{n} T_{j_m} + n\tau$, with each T_{j_m} being some member of $\{T_1, \ldots, T_k\}$. This contradicts that $x_t(\bar{\phi}, \bar{\gamma}) \in V_2$, for all $t \geq 0$. Hence (76) holds.

Now the conclusion follows from Theorem 5 in Smith and Zhao (2001), applied with the generalized distance function $\tilde{p} : C_+ \to \mathbb{R}$, $\tilde{p}(\phi) = \min_{i=3,4} \min_{\theta \in [-\tau, 0]} \phi_i(\theta)$.

iv). It follows from *ii)* and *iii)*.

□

References

Abedon ST, Herschler TD, Stopar D (2001) Bacteriophage latent-period evolution as a response to resource availability. Appl Environ Microbiol 67(9):4233–4241

Ananworanich J, Dubé K, Chomont N (2015) How does the timing of antiretroviral therapy initiation in acute infection affect HIV reservoirs? Curr Opin HIV AIDS 10(1):18

Bai F, Huff KE, Allen LJ (2019) The effect of delay in viral production in within-host models during early infection. J Biol Dyn 13(sup1):47–73

Beretta E, Kuang Y (1998) Modeling and analysis of a marine bacteriophage infection. Math Biosci 149(1):57–76

Beretta E, Kuang Y (2001) Modeling and analysis of a marine bacteriophage infection with latency period. Nonlinear Analysis: Real World Appl 2(1):35–74

Beretta E, Solimano F, Tang Y (2002) Analysis of a chemostat model for bacteria and virulent bacteriophage. Discrete and Continuous Dynamical Systems - Series B

Browne C (2016) Immune response in virus model structured by cell infection-age. Math Biosci Eng 13(5):887–909

Buckheit RW, Siliciano RF, Blankson JN (2013) Primary cd8+ t cells from elite suppressors effectively eliminate non-productively HIV-1 infected resting and activated cd4+ t cells. Retrovirology 10(1):68

Childs LM, Held NL, Young MJ, Whitaker RJ, Weitz JS (2012) Multiscale model of crispr-induced coevolutionary dynamics: diversification at the interface of Lamarck and Darwin. Evol Int J Organic Evol 66(7):2015–2029

Chomont N, El-Far M, Ancuta P, Trautmann L, Procopio FA, Yassine-Diab B, Boucher G, Boulassel MR, Ghattas G, Brenchley JM et al (2009) HIV reservoir size and persistence are driven by t cell survival and homeostatic proliferation. Nat Med 15(8):893

Ciupe SM, Heffernan JM (2017) In-host modeling. Infect Disease Model 2(2):188–202

Dahari H, Shudo E, Ribeiro RM, Perelson AS (2009) Modeling complex decay profiles of hepatitis B virus during antiviral therapy. Hepatology 49(1):32–38

Díaz-Muñoz SL, Koskella B (2014) Bacteria-phage interactions in natural environments. Adv Appl Microbiol 89:135–183

Engelborghs K, Luzyanina T, Roose D (2002) Numerical bifurcation analysis of delay differential equations using DDE-BIFTOOL. ACM Trans Math Software 28(1):1–21

Engelborghs K, Luzyanina T, Samaey G (2001) DDE-BIFTOOL v. 2.00: A Matlab package for bifurcation analysis of delay differential equations. Tech. Rep., Department of Computer Science, K.U.Leuven, Belgium

Ermentrout B (2002) Simulating, analyzing, and animating dynamical systems: a guide to XPPAUT for researchers and students. SIAM

Fan G, Wolkowicz GSK (2021) Chaotic dynamics in a simple predator–prey model with discrete delay. Discrete Contin Dyn Syst Ser B 26(1):191–216. 10.3934/dcdsb.2020263, http://aimsciences.org//article/id/98219fc8-a50c-488b-a1c3-3afd1764f077

Goldfarb T, Sberro H, Weinstock E, Cohen O, Doron S, Charpak-Amikam Y, Afik S, Ofir G, Sorek R (2015) Brex is a novel phage resistance system widespread in microbial genomes. EMBO J 34(2):169–183

Goyal A, Ribeiro R, Perelson A (2017) The role of infected cell proliferation in the clearance of acute HBV infection in humans. Viruses 9(11):350
Gulbudak H, Martcheva M (2013) Forward hysteresis and backward bifurcation caused by culling in an avian influenza model. Math Biosci 246(1):202–212
Gulbudak H, Weitz JS (2016) A touch of sleep: biophysical model of contact-mediated dormancy of archaea by viruses. Proc R Soc B 283(1839):20161037
Gulbudak H, Weitz JS (2019) Heterogeneous viral strategies promote coexistence in virus-microbe systems. J Theor Biol 462:65–84
Hale J, Lunel S (1993) Introduction to functional differential equations. Springer-Verlag, New York
Han Z, Smith HL (2012) Bacteriophage-resistant and bacteriophage-sensitive bacteria in a chemostat. Math Biosci Eng 9(4):737
Ishida Y, Chung TL, Imamura M, Hiraga N, Sen S, Yokomichi H, Tateno C, Canini L, Perelson AS, Uprichard SL et al (2018) Acute hepatitis B virus infection in humanized chimeric mice has multiphasic viral kinetics. Hepatology 68(2):473–484
Jansen V, Sigmund K (1998) Shaken not stirred: on permanence in ecological communities. Theor Popul Biol 54:195–201
Jover LF, Cortez MH, Weitz JS (2013) Mechanisms of multi-strain coexistence in host-phage systems with nested infection networks. J Theor Biol 332:65–77
Kakizoe Y, Nakaoka S, Beauchemin CA, Morita S, Mori H, Igarashi T, Aihara K, Miura T, Iwami S (2015) A method to determine the duration of the eclipse phase for in vitro infection with a highly pathogenic SHIV strain. Sci Rep 5:10371
Labrie SJ, Samson JE, Moineau S (2010) Bacteriophage resistance mechanisms. Nat Rev Microbiol 8(5):317
Levin BR, Stewart FM, Chao L (1977) Resource-limited growth, competition, and predation: a model and experimental studies with bacteria and bacteriophage. Am Nat 111(977):3–24
Loh B, Kuhn A, Leptihn S (2019) The fascinating biology behind phage display: filamentous phage assembly. Mol Microbiol 111(5):1132–1138
Maple: Release 2020.2. Maplesoft, a division of Waterloo Maple Inc., Waterloo, Ontario (2020)
MATLAB: (R2020a). The MathWorks Inc., Natick, Massachusetts (2020)
Northcott K, Imran M, Wolkowicz GSK (2012) Competition in the presence of a virus in an aquatic system. J Math Biol 64:1043–1086
Pinzone MR, VanBelzen DJ, Weissman S, Bertuccio MP, Cannon L, Venanzi-Rullo E, Migueles S, Jones RB, Mota T, Joseph SB et al (2019) Longitudinal HIV sequencing reveals reservoir expression leading to decay which is obscured by clonal expansion. Nature Commun 10(1):1–12
Pituk M (2018) A perron type theorem for positive solutions of functional differential equations. Electron J Qualit Theory Differ Equ 57:1–11
Ploss M, Kuhn A (2010) Kinetics of filamentous phage assembly. Phys Biol 7(4):045002
Rong L, Perelson AS (2009) Asymmetric division of activated latently infected cells may explain the decay kinetics of the HIV-1 latent reservoir and intermittent viral blips. Math Biosci 217(1):77–87
Rouzine IM, Weinberger AD, Weinberger LS (2015) An evolutionary role for HIV latency in enhancing viral transmission. Cell 160(5):1002–1012
Salceanu P (2011) Robust uniform persistence in discrete and continuous dynamical systems using Lyapunov exponents. Math Biosci Eng 8(3):807–825
Salceanu P, Smith HL (2009) Lyapunov exponents and persistence in discrete dynamical systems. Discrete Contin Dyn Syst Ser B 12(1):187–203
Smith H, Zhao XQ (2001) Robust persistence for semidynamical systems. Nonlinear Anal Theory Methods Appl 47(9):6169–6179
Smith HL (1995) Monotone dynamical systems, an introduction to the theory of competitive and cooperative systems. Math Surv Monographs 41
Smith HL (2011) An introduction to delay differential equations with applications to the life sciences, vol 57. Springer, New York
Smith HL, De Leenheer P (2003) Virus dynamics: a global analysis. SIAM J Appl Math 63(4):1313–1327
Smith HL, Thieme HR (2011) Dynamical systems and population persistence, vol 118. American Mathematical Soc
Smith HL, Thieme HR (2012) Persistence of bacteria and phages in a chemostat. J Math Biol 64(6):951–979
Stewart FM, Levin BR (1984) The population biology of bacterial viruses: why be temperate. Theor Popul Biol 26(1):93–117

Teslya A, Wolkowicz GSK (2020) Dynamics of a predator-prey model with distributed delay to represent the conversion process or maturation. Differ Equ Dyn Syst. 10.1007/s12591-020-00546-4, https://rdcu.be/b6gOy

Violari A, Cotton MF, Kuhn L, Schramm DB, Paximadis M, Loubser S, Shalekoff S, Dias BDC, Otwombe K, Liberty A et al (2019) A child with perinatal HIV infection and long-term sustained virological control following antiretroviral treatment cessation. Nature Commun 10(1):1–11

Weitz JS (2016) Quantitative viral ecology: dynamics of viruses and their microbial hosts, vol 73. Princeton University Press, Princeton

Weitz JS, Li G, Gulbudak H, Cortez MH, Whitaker RJ (2019) Viral invasion fitness across a continuum from lysis to latency. Virus Evol 5(1):vez006

Wodarz D (2001) Viruses as antitumor weapons: defining conditions for tumor remission. Cancer Res 61(8):3501–3507

Wolkowicz GSK, Xia H (1997) Global asymptotic behavior of a chemostat model with discrete delays. SIAM J Appl Math 57:1019–1043

Wolkowicz GSK, Xia H, Ruan S (1997) Competition in the chemostat: a distributed delay model and its global asymptotic behavior. SIAM J Appl Math 57(5):1281–1310

Terms and Conditions

Springer Nature journal content, brought to you courtesy of Springer Nature Customer Service Center GmbH ("Springer Nature").

Springer Nature supports a reasonable amount of sharing of research papers by authors, subscribers and authorised users ("Users"), for small-scale personal, non-commercial use provided that all copyright, trade and service marks and other proprietary notices are maintained. By accessing, sharing, receiving or otherwise using the Springer Nature journal content you agree to these terms of use ("Terms"). For these purposes, Springer Nature considers academic use (by researchers and students) to be non-commercial.

These Terms are supplementary and will apply in addition to any applicable website terms and conditions, a relevant site licence or a personal subscription. These Terms will prevail over any conflict or ambiguity with regards to the relevant terms, a site licence or a personal subscription (to the extent of the conflict or ambiguity only). For Creative Commons-licensed articles, the terms of the Creative Commons license used will apply.

We collect and use personal data to provide access to the Springer Nature journal content. We may also use these personal data internally within ResearchGate and Springer Nature and as agreed share it, in an anonymised way, for purposes of tracking, analysis and reporting. We will not otherwise disclose your personal data outside the ResearchGate or the Springer Nature group of companies unless we have your permission as detailed in the Privacy Policy.

While Users may use the Springer Nature journal content for small scale, personal non-commercial use, it is important to note that Users may not:

1. use such content for the purpose of providing other users with access on a regular or large scale basis or as a means to circumvent access control;
2. use such content where to do so would be considered a criminal or statutory offence in any jurisdiction, or gives rise to civil liability, or is otherwise unlawful;
3. falsely or misleadingly imply or suggest endorsement, approval , sponsorship, or association unless explicitly agreed to by Springer Nature in writing;
4. use bots or other automated methods to access the content or redirect messages
5. override any security feature or exclusionary protocol; or
6. share the content in order to create substitute for Springer Nature products or services or a systematic database of Springer Nature journal content.

In line with the restriction against commercial use, Springer Nature does not permit the creation of a product or service that creates revenue, royalties, rent or income from our content or its inclusion as part of a paid for service or for other commercial gain. Springer Nature journal content cannot be used for inter-library loans and librarians may not upload Springer Nature journal content on a large scale into their, or any other, institutional repository.

These terms of use are reviewed regularly and may be amended at any time. Springer Nature is not obligated to publish any information or content on this website and may remove it or features or functionality at our sole discretion, at any time with or without notice. Springer Nature may revoke this licence to you at any time and remove access to any copies of the Springer Nature journal content which have been saved.

To the fullest extent permitted by law, Springer Nature makes no warranties, representations or guarantees to Users, either express or implied with respect to the Springer nature journal content and all parties disclaim and waive any implied warranties or warranties imposed by law, including merchantability or fitness for any particular purpose.

Please note that these rights do not automatically extend to content, data or other material published by Springer Nature that may be licensed from third parties.

If you would like to use or distribute our Springer Nature journal content to a wider audience or on a regular basis or in any other manner not expressly permitted by these Terms, please contact Springer Nature at

onlineservice@springernature.com